SECONDARY ION MASS SPECTROMETRY ANALYSIS OF VESICLE MEMBRANES USING NANO-PROJECTILES

A Dissertation

By

DMITRIY STANISLAVOVICH VERKHOTUROV

Submitted to the Office of Graduate and Professional Studies of
Texas A & M University
in partial fulfillment of the requirements for the degree of

DOCTOR OF PHILOSOPHY

Chair of Committee,	Emile A. Schweikert
Committee Members,	Robert Burghardt
	David H. Russell
	Yanan Tian
Head of Department,	Ivan Rusyn

December 2020

Major Subject: Toxicology

ABSTRACT

Nanoscale toxins and pollutants such as ultrafine particles and metals from the environment can enter the human body and interact with host membrane proteins disrupting normal metabolism either directly or by causing changes to host membrane organization. It is important to shed light on the mechanism of action of these nanoscale toxins by studying their target proteins and how the host membrane protein-lipid raft complex interactions are modified. To do so there needs to be a technique which can stochastically probe nano-volumes on the membrane surface to characterize protein co-localization on the macroscale. Nano-projectile bombardment secondary ion mass spectrometry (NP-SIMS) is one such technique which uses single gold cluster nano-projectiles as nano-probes to provide information on co-localization of moieties within ~20 nm on the surface by analyzing the related co-emitted species. The purpose of the present work was to develop methodology to apply this unique technique to the study of surface proteins and to test it on vesicle membranes. In order to do so, several challenges were overcome.

The first challenge is that, in practice, upon nano-projectile impact, only molecules and fragments up to ~1500 Da ionize efficiently to be detected thus proteins that are larger in size must be tagged. Several commercially available tagging approaches were tested: lanthanide-chelated polymer scaffold, metal nanoparticle and halide-containing small molecules. Model experiments were performed for each approach with a sub-single layer of antibody conjugated to a representative tag. ^{142}Nd-chelated X8 polymer scaffold and 5 nm PEG-coated gold nanoparticle tags were conjugated to rituximab antibody and covalently attached onto a functionalized silicon

wafer. It was found that the tags utilizing the polymer scaffold did not have a strong enough signal to be used with biological samples due to the lanthanide atom density in direct proximity of the antibody being low. The 5 nm gold nanoparticle tag had its signal suppressed because of the PEG cap and antibody layers that inhibited tag-related ion emission from the metal core and thus also did not have the required sensitivity for biological samples. BHHTEGST, eosin and erythrosine, which contained fluorine, bromine and iodine halide tags respectively, could be conjugated directly at the surface of the antibody avoiding the issues of the other two tagging approaches. Thus halide tags were chosen for downstream experiments.

Model samples approximating membrane surfaces which contained covalently attached single layers of Ab conjugated BHHTEGST, eosin or erythrosine tags were prepared and analyzed with NP-SIMS. Based on the yields (ions detected per impact) obtained for fluoride and iodide, the “decision limits” were calculated for BHHTEGST and erythrosine tags respectively. The “decision limit” for erythrosine was between 96 and 236 tagged proteins per μm^2 of a membrane. For BHHTEGST, the “decision limit” was between 280 and 685 tagged proteins per μm^2 of a membrane. The bromide ions characteristic of eosin were interfered by phosphate-related ions.

A proof-of-concept experiment was performed where the halide-containing molecular tagging approach was applied to detection of podocin on the surface of urine-derived Evs. Briefly, Evs were attached to a functionalized ITO surface via poly-L-lysine (PLL) and labeled with anti-podocin Abs conjugated to erythrosine. Erythrosine contains the iodine tag. Tagged podocin protein was successfully detected. Next, detection of two co-localized proteins on Evs was tested. CD63 and CD81 were tagged on Evs with

erythrosine and BHHTEGST respectively. Tagged Evs were then attached as a sub-single layer to a functionalized ITO surface using electrostatic interactions and dehydrated. We were able to successfully detect co-localized tagged CD63 and CD81 in 0.003% of the impacts.

Now that a viable tagging approach was chosen that provides the detection sensitivity required to be able to study at least two tagged proteins on biological surfaces, the next objective was to examine the limits of co-localization of tagged proteins on a single layer model surface similar to a membrane. A model experiment was performed where three halide-containing tags (BHHTEGST, eosin and erythrosine) were conjugated to antibody, mixed equimolarly and covalently attached to a functionalized surface. It was shown that it is possible to detect all three tags in a single projectile impact. Furthermore, degree of co-localization analysis found that the three-tag model surface is inhomogeneous on the scale of emission from a single projectile impact of 20 nm in diameter. The fluctuations in co-localization were attributed to the differences in hydrophobicity and functional groups between the tags. Tags containing BHHTGEST chelated with different lanthanide metals have the same hydrophobicity and chemical properties and were thus used to avoid inhomogeneity at the nanoscale. It was demonstrated for a two-tag (Eu and Sm) model experiment, that tagged Abs attached in a random manner on the surface without density fluctuations detected at the ~20 nm scale.

Future experiments should focus on extending multiplexing capability to the approach as well as incorporating a mapping feature which can determine the location of each impact with sub-micron special resolution. It is possible to use laser post-

ionization with BHHTEGST- chelated lanthanide tags in order to enable extensive multiplexing as there are 55 lanthanide isotopes available. These can be ionized with a 193 nm ArF excimer commercially available laser. Additionally, the nano-projectile parameters such as energy, size and momentum can be adjusted to change the nano-volume of emission and detection sensitivity required for a particular analyte. Assuming the above challenges can be overcome, NP-SIMS may then be able to provide unique insights into how toxins affect host membrane protein-lipid raft complexes.

ACKNOWLEDGMENTS

I would like to especially thank my parents, Stanislav Verkhoturov and Firuza Badamshina, for everything they have done for me.

I would also like to thank the following: my advisor, Dr. Schweikert, for his mentorship; my committee members Dr. Burghardt, Dr. Russell, and Dr. Tian; our collaborators, especially Dr. Revzin; Dr. Barondeau for letting me use his equipment and lab space for my experiments; and last but not least Jesse Sandoval for BHHTEGST and discussions.

CONTRIBUTORS AND FUNDING SOURCES

Contributors

This work was supported by a dissertation committee consisting of Professors Emile A. Schweikert and David H. Russell of the Department of Chemistry and Professors Robert Burghardt and Yanan Tian of the Department of Veterinary Medicine.

The functionalized surfaces analyzed were provided by Professor Alex Revzin at Mayo Clinic. BHHTEGST was prepared by Jesse Sandoval with the help of Professor David E. Bergbreiter's lab.

All other work conducted for the dissertation was completed by the student independently.

Funding Sources

Graduate study was supported by grant R01 GM123757-01 from the National Institute of Health.

TABLE OF CONTENTS

Page

ABSTRACT ii

ACKNOWLEDGMENTS vi

CONTRIBUTERS AND FUNDING SOURSCES vii

TABLE OF CONTENTS viii

LIST OF FIGURES x

LIST OF TABLES xiii

1. INTRODUCTION 1

1.1 References 4

2. LITERATURE REVIEW 5

2.1 Classical Approaches 6
2.2 Super-Resolution Microscopy 6
2.3 Mass Spectrometry 7
2.4 Summary of Techniques Discussed 11
2.5 Extracellular Vesicles (EVs) 12
2.6 References 14

3. EXPERIMENTAL 15

3.1 Tagging 15
3.2 Model Surface Preparation 16
3.3 Extracellular Vesicles (EVs) Preparation 17
3.4 Instrument 17
3.5 More Efficient Larger Projectile $(Au_{2800})^{8+}$ 21
3.6 Beam Tuning, Data Acquisition and Analysis 24
3.7 References 27

4. EVALUATION OF TAGS FOR NP-SIMS 28

4.1 Chelated Polymer Scaffold Tags 28
4.2 NP Tagging Approach 37

5. ULTRA-SENSITIVE DETECTION OF TAGGED PROTEINS IN VESICLE MEMBRANES WITH NANO-PROJECTILE SECONDARY ION MASS SPECTROMETRY 46

5.1 Introduction 46

5.2 Experiment and Methods 48
5.3 Results and Discussion 57
5.4 Conclusions 69
5.5 References 71

6. METHODOLOGY FOR CO-LOCALIZATION 74

6.1 Introduction 74
6.2 Results and Discussion 75
6.3 Conclusions 89
6.4 References 91

7. CONCLUSIONS 92

7.1 References 97

APPENDIX 98

LIST OF FIGURES

FIGURE Page

3.1. Diagram of the custom-built NP-SIMS instrument consisting of a liquid metal ion source (LMIS) and a reflectron TOF mass spectrometer using an 8 anode microchannel plate (MCP) detector. Magnetic prism diverts electrons in negative mode that can be used as a start signal 20

3.2. Wien filter scan of the possible projectiles produced by the liquid metal ion source as well as representative time-of-flight measurements of n/q=100 or $(Au_{400})^{4+}$ and n/q=350 or $(Au_{2800})^{8+}$..... 22

3.3. Transmission electron micrographs of impact craters on 10 nm amorphous carbon. (A) Impacts of 520 keV Au_{400}^{4+} with a 45° impact angle, scale bar 50 nm. (B) Impacts of 1040 keV Au_{2800}^{8+} with a 45° impact angle, scale bar 100 nm. 23

4.1. Maxpar isotopic metal tag conjugation..... 29

4.2. Functionalization of Si wafer and attachment of conjugated antibodies for the model experiment..... 31

4.3. Negative ion mass spectrum of APTES/GA functionalized Si wafer (Sample 1) using 520 keV Au_{400}^{4+} projectiles..... 33

4.4. Negative ion mass spectrum of APTES/GA functionalized Si wafer with attached antibody (Ab) (Sample 2) using 520 keV Au_{400}^{4+} projectiles..... 34

4.5. Negative ion mass spectrum of APTES/GA functionalized Si wafer with attached antibody (Ab) conjugated to Nd/polymer tag (Sample 3) taken using negative mode and 520 keV Au_{400}^{4+} projectiles..... 35

4.6. a) Positive mode total mass spectrum taken using 440 keV Au_{400}^{4+} projectiles showing the NdO^+ peak. b) Mass spectrum showing co-emission with NdO. Nd tag antibody conjugate coverage was 10%..... 36

4.7. Experimental concept of using NP tags with NP-SIMS method..... 38

4.8. Model experimental design for AuNP-Ab tagging. ITO glass was functionalized by mouse antibodies inside of a PDMS well and then tagged by AuNPs to model cell surface conditions. 40

FIGURE Page

4.9. Mass spectra of AuNPs conjugated to mouse Ab. a) Area of the sample where AuNP-Ab were deposited (inside the PDMS well). b) An area of the sample outside the PDMS well..... 42

4.10. a) Illustration of the NP-Ab conjugates which were prepared. b) Depiction of how the NP-Ab conjugate can be improved to increase signal from the tag with a thinner cap and fewer attached Abs 44

5.1. Tagging approach. a) Molecules conjugated to rituximab antibody (Ab) are BHHTEGST (fluoride tag), eosin (bromide tag) and erythrosine (iodide tag). b) Sketch of the model surface..... 49

5.2. Sketch of emission volume stimulated by single projectile impact on a single tag model surface 51

5.3. Sketch of EV sample design. Podocin on EVs was tagged with corresponding Ab conjugated to erythrosine tag 53

5.4. Schematic of custom-made NP-SIMS instrument..... 55

5.5. The mass spectrum taken from the model sample of erythrosine-Ab conjugates (I tag) with direct covalent attachment on functionalized Au coated Si wafer. a) mass range of 0-100 amu, b) mass range of 100-300 amu, c) mass range of 300-1300 amu 58

5.6. The mass spectrum taken from the model sample of Eosin-Ab conjugates (Br tag) with direct covalent attachment on a functionalized Au coated Si wafer. a) mass range of 0-100 amu, b) mass range of 100-310 amu 59

5.7. The mass spectrum taken from the model sample of BHHTEGST-Ab conjugates (F^- tag) with direct covalent attachment on functionalized Au coated Si wafer. a) mass range of 0-100 amu, b) mass range of 100-300 amu..... 60

5.8. SEM micrograph of the tagged EV sample. The round shaped objects are EVs. The small crystals at the surface are likely salt inclusions..... 64

5.9. a) Mass spectra from the proof-of-concept EV experiment. The top (blue) mass spectrum is for EVs, which were tagged by erythrosine-Ab. b) Comparison of the peaks of I^- for all mass spectra 66

FIGURE Page

5.10. Mass spectra of two-tag EV experiment. (a) Shows comparison of F^- peak for EVs tagged with BHHTGEST-antiCD81-Ab, EVs tagged with erythrosine-antiCD63-Ab and BHHTGEST tagged CD Anti-CD81 Ab and untagged EVs. (b) Comparison of the 3 samples listed above but for I^- peak. 68

6.1. Mass spectrum of equimolar mixture model surface (three tags). a) Mass spectrum for selected projectile impacts where all three tags were detected (coincidence mass spectrum). b) Total mass spectrum for all projectile impacts. Probing area of each individual projectile impact was ~20 nm in diameter 76

6.2. Sketch of BHHTEGST molecular tag chelated with Eu atom 82

6.3. Selected areas of the mass spectrum of sample 1 (Eu-BHHTEGST-Ab). The characteristic peaks of chelated tag molecules (top, red) are compared with the peaks from the same mass areas for control sample (bottom black) of BHHTEGST-Ab (no chelated Eu) 85

6.4. Selected areas of the mass spectrum of sample 2 (Sm-BHHTEGST-Ab). The characteristic peaks of chelated tag molecules (top, pink) are compared with the peaks from the same mass areas for control sample of BHHTEGST-Ab (no chelated Sm) 86

6.5. Selected areas of the mass spectrum of sample 3 (mix of Eu-BHHTEGST-Ab and Sm-BHHTEGST-Ab). The characteristic peaks of chelated tag molecules (top, green) are compared with the peaks from the same mass areas for the control sample (bottom, black) of BHHTEGST-Ab (no chelated Eu and Sm) 87

LIST OF TABLES

TABLE Page

2.1 Summary of analysis methods. 12

3.1 Comparison of tagging approaches used in the study 16

5.1. Characteristic ions detected for each tag conjugated to Ab. 61

5.2. Yields (ions detected per impact) for each halide ion on model single layer surfaces. 61

5.3. Surface coverages for each sample..... 63

6.1. Co-localization factor for double and triple co-localizations of antibodies 79

6.2. Coverage coefficients, K, for samples 1-3 88

1. INTRODUCTION

The body is constantly exposed to nanoscale toxins which make their way inside either through the lungs, ingestion or skin contact and can disrupt proper function of surface proteins either on host cells or mutualistic microbiota.[1] This is especially pertinent in the modern era where human activity produces increasing amounts of pollutants.[2] The recent development of nanotechnologies and their application to industry has also resulted in an increase in ultrafine particles in the environment. Ultrafine particles are particulate matter which can range between a few nm to 100 nm in size.[2] Due to their small size these particles can make their way into the body and even penetrate into the bloodstream. A portion of them is chemically active or can be activated by the body's clearing systems. Foreign chemically active particles will react with host biomolecules disrupting normal processes including those on the cell membranes. Alternatively, these toxins can initiate harmful changes such as altering membrane composition of cells and vesicles. It is important to study the effects of these nanoscale toxins as well as to shed light on their mechanism of action. Specifically, protein and lipid targets of particular toxins need to be elucidated and changes to membrane composition and membrane protein-protein interactions of host cells examined.

An eminently suitable technique for determining the chemical composition of surfaces at the nanoscale is secondary ion mass spectrometry (SIMS). This technique enables monitoring of the emission of characteristic ions which are generated by impacts of primary projectile ions. Projectile ions used range from atomic ions to atomic or molecular clusters. Atomic ion beams can be tightly focused which allows for high

spatial resolution (down to 33 nm).[3] However, cluster projectiles are more efficient than equal velocity atomic ions. Indeed, the secondary ion (SI) yield obtained with poly-atomic projectiles containing up to 9 atoms increases in a supra-linear mode.[4] As cluster size increases towards nanoparticles, the SI yield still grows linearly at equal velocities.[5] Moreover, clusters and nanoparticles are the most tightly focused ensembles of atoms with the unique ability to deposit the highest density of energy into the impact solid. Simultaneous impact of cluster atoms generates a high-density collision cascade which in turn results in crater formation and an abundant sputtering process. The high-density cascade generates correlated pulses toward the surface promoting efficient ejection of molecules and molecular fragments.

The most advanced SIMS concept for nanoscale analysis uses nanoparticle projectiles as nanoprobes to inspect the surface layer stochastically with millions of nano-projectile impacts where the secondary ions are detected separately for each impact.[6,7] This event-by-event technique termed nano-projectile SIMS (NP-SIMS) enables stochastic analysis of nano-volumes obtained via single nano-projectile impacts. The approach was applied to characterize lipids and lipid-related fragments in mammalian brain tissues using a gold nano-projectile, specifically Au_{400}^{4+} accelerated to 520 keV.[8,9] In the present study, we examine the application of NP-SIMS to probe proteins in cell and vesicle membranes. Investigation of proteins in a nano-volume requires detection sensitivity at the atto or sub-attomole level. Additionally, the volume of the analyte versus the volume sampled is a key concern. Given these considerations, the experimental effort focused on applying as massive a projectile as possible to maximize nano-volume assayed and detection sensitivity. Among the common large

cluster projectiles (e.g. Ar_{2000}^{+}, $(H_2O)_{7000}^{+}$, $(CO_2)_{2000}^{+}$) accelerated up to 130 kV, Au_{2800}^{8+}, used in the present study, has been shown to provide the highest ion yields.[10] Moreover, the Au_{2800}^{8+} nano-projectile has an emission volume[9] of 20×20×10 nm^3 which is suitable for probing co-localized moieties of a protein-lipid raft membrane complex.[11] It is important to note that, with NP-SIMS, in practice only organic species up to ~1500 Da ionize effectively. Thus, tagging is required to achieve selectivity of detection for most proteins.

In the subsequent chapters of the dissertation the following topics are addressed: (1) literature review concerning methods of tagged surface protein analysis at the nanoscale and an overview of extracellular vesicles (EVs), which served as test specimens; (2) descriptions of custom-made NP-SIMS device and methodology, tagging and sample preparation; (3) feasibility testing of chelated polymer scaffold and nanoparticle tagging methods for NP-SIMS; (4) application of NP-SIMS for ultra-sensitive detection of tagged podocin as well as detection of co-localized tagged CD63 and CD81 proteins on extracellular vesicles (EVs); (5) development of methodology to study co-localization of tagged antibodies using model surfaces; (6) conclusions for the study as a whole.

1.1 References

(1) T.-Y. Wong, Journal of food and drug analysis **25**, 235 (2017).

(2) P. J. A. Borm, Inhalation Toxicology **14**, 311 (2002).

(3) C. Lechene, F. Hillion, G. McMahon, D. Benson, A. M. Kleinfeld, J. P. Kampf, D. Distel, Y. Luyten, J. Bonventre, D. Hentschel, K. M. Park, S. Ito, M. Schwartz, G. Benichou, G. Slodzian, Journal of Biology **5**, 20 (2006).

(4) M. G. Blain, S. Della-Negra, H. Joret, Y. Le Beyec, and E. A. Schweikert, Phys. Rev. Lett. **63**, 1625 (1989).

(5) H. H. Andersen, A. Brunelle, S. Della-Negra, J. Depauw, D. Jacquet et al., Phys. Rev. Lett. **80**, 5433 (1998).

(6) M. A. Park, K. A. Gibson, K. Quinones, and M. A. Schweikert, Science **25**, 988 (1990).

(7) M. J. Van Stipdonk, E. A. Schweikert, and M. A. Park, J. Mass Spectrom. **32**, 1151 (1999).

(8) F. A. Fernandez-Lima, J. Post, J. D. DeBord, M. J. Eller, S. V. Verkhoturov, S. Della-Negra, A. S. Woods, E. A. Schweikert, Anal. Chem. **83**, 8448 (2011).

(9) F. A. Fernandez-Lima, J. D. DeBord, E. A. Schweikert, S. Della-Negra, K. A. Kellersberger, M. Smotherman, Surf. Interface Anal. **45**, 294 (2013).

(10) M. J. Eller, A. Vinjamuri, B. E. Tomlin, E. A. Schweikert, Anal. Chem. **90**, 12692 (2018).

(11) K. Simons and D. Toomre, Nat Rev Mol Cell Biol **1**, 31 (2000).

2. LITERATURE REVIEW

Initially biological studies of organisms began with direct macroscopic observation. It was found that an organism consists of multiple organs each performing their own functions. Emergence of new technologies allowed scientists to delve into the microscopic world and it was discovered that each organ consists of multiple specialized tissues which are made out of many types of cells, the basic unit of life. Digging deeper, at the nano-level it was found that a cellular membrane consists of a lipid bilayer with embedded or attached biomolecules such as proteins and carbohydrates that form complexes and nano-domains which are crucial to cell function and cross talk. As we find out more about all the mechanisms and pathways that determine cell fate, it becomes clear how intricate and complex the systems are with many of the signaling pathways all affecting and balancing each other. Thus arose the need to study the composition and interaction of multiple biomolecules on cell surfaces simultaneously. This is a still evolving field where the research and biomedical communities are constantly seeking to improve the current resolution and multiplexing capabilities while trying to decreases analysis times. Specifically, interaction and thus co-localization of important biomolecules on particular localized areas of the cell surface can play a big role in their biological function. Techniques relevant for multi-tag and co-localization studies are summarized below. Also included in this chapter is a brief review of description of the characteristics of extracellular vesicles (EVs), which served as test specimens.

2.1 Classical Approaches

Classical approaches to this problem include immunohistochemistry and fluorescence microscopy. Briefly, proteins of interest would be tagged with a primary antibody which subsequently would be tagged with an anti-primary secondary antibody that is conjugated to a reporter to image their location. Immunohistochemistry is labor intensive for multiplexing because one has to tag and image each protein one at a time. However, using a fluorescent reporter, multiple tags can be used simultaneously and the upper limit is about ten to twelve due to wavelength interference[1].

2.2 Super-Resolution Microscopy

Super-resolution microscopy is a technique which uses fluorescent tags in conjunction with techniques designed to overcome the optical diffraction limit to improve the resolution of fluorescence microscopy down to 50 nm[2]. Among the different super-resolution imaging techniques (near-field scanning optical microscopy (NSOM), stimulated emission depletion microscopy (STED), photoactivated localization microscopy (PALM), stochastic optical reconstruction microscopy (STORM)), PALM/STORM provide the best lateral resolution and are most commonly used for biological applications[2]. The basic principle of the technique uses sequentially photoactivated fluorophore tags to reconstruct their positions with sub-diffraction-limit resolution. Using this technique different biological targets such as tissues, cells and extracellular vesicles (EVs) have been studied. The advantage of the technique is that one can image tagged biomolecules with nanometric resolution, however, it is currently limited by the number of tags (up to 3) that can simultaneously be used as well as its labor-intensive nature[2].

2.3 Mass Spectrometry

Conversely, mass spectrometry-based techniques allow the usage of potentially up to 40 tags[3] simultaneously. The following are the three main approaches that have been used for biological studies and are discussed below: nanoscale secondary ion mass spectrometry (nanoSIMS), laser-ablation inductively coupled plasma mass spectrometry[4] (LA-ICP-MS) and single nano-projectile bombardment secondary ion mass spectrometry (NP-SIMS).

In all three methods, antibody tags are used which are conjugated to isotopically enriched metals or metal oxides that do not have isobaric interference with other ions emitted from the sample including other tags. One conjugation approach commonly used is binding the metal atoms to a polymer scaffold through a chelator and then using maleimide chemistry to attach the polymer to free cysteine groups on the antibody of interest[5]. Another tagging approach used with mass spectrometry is isotope labeling where isotopes with low natural abundance such as ^{13}C, ^{15}N, and ^{18}O are introduced and tracked.

2.3.1 NanoSIMS

NanoSIMS uses a focused beam of primary ions such as cesium or oxygen to bombard the target surface which contains isotopically tagged molecules of interest. Ionized tags are then detected and an ion image can be reconstructed showing the localization of the tagged species. The advantage of nanoSIMS is high resolution as the primary beam can be focused down to 33 nm[6], however, the drawback is that molecular information is lost and only atomic species and small molecular fragments are detected. For this reason, a tagging approach using isotopic labels is required for biological

applications. Additionally, it is important to note that the sample has to be under vacuum conditions and thus biological samples have to be fixed via crosslinking agents and dehydrated (all mass spectrometry techniques discussed here use fixed and dehydrated samples).

2.3.1.1 Multi-Isotope Imaging Mass Spectrometry (MIMS)

One approach to using nanoSIMS in biological studies is introducing isotopically labeled metabolites such as ^{13}C, ^{15}N,^{18}O or labeled lipids, amino acids and nucleic acids to study their respective metabolic pathways[6]. This method has been successfully used to research critical biological processes such as lipid transport, nitrogen fixation, protein renewal, nucleotide incorporation, etc[6]. Using this method of tagging allows for application of highly focused beams with resolution down to 33 nm, however, the types of biological studies that can be done are limited by the fact that you have to incorporate isotopically enriched tags into the object of study while preventing incorporation of natural isotopes at the same time. The number of tags is also limited by the number of isotopes available that can be used in such a manner.

2.3.1.2 Multiplexed Ion Beam Imaging (MIBI)

MIBI[7] involves using a highly focused oxygen primary beam produced by a duoplasmatron source to bombard the sample surface yielding secondary ions. Using oxygen primary ions promotes the ionization of positive species (such as metal tags) by scavenging electrons. The emitted ions from each pixel are separated using a magnetic sector mass analyzer with seven detectors (number of detectors used simultaneously depends on the instrument used). The beam scans small overlapping sections of the sample surface with each scan able to record information on up to seven of the metal

tags. To gather information on more tagged molecules, additional sequential scans have to be performed on the same area. The beam spot size determines the smallest pixel size that can be used which in turn becomes the limiting factor on the maximum resolution. Using the overlapping parts of each scan section, an overall total map can be constructed for the entire sample surface. The advantages of this method include multiplexing capability while maintaining a relatively high resolution of 200 nm. In addition, comparing signal intensities between the different pixels can provide relative quantification of a particular tagged molecule across the sample surface with sub-cellular nanoscale resolution. The current difficulties with the MIBI method include the progressively increasing scanning time when stacking high resolution and each additional set of tags compared to the number of detectors used. However, these can be partially mitigated by using higher density tags (such as isotopically enriched nanoparticles) where pixel dwell times can be reduced by orders of magnitude and by increasing the number of detectors where one can detect more tags per scan. Also, there have been improvements in the oxygen plasma sources available decreasing their spot size while improving brightness. The above issues limit MIBI's use where high throughput is required.

2.3.2 Laser Ablation Inductively Coupled Plasma Mass Spectrometry (LA-ICP-MS)

Overall, while MIBI is a powerful technique that combines multiplexing and high resolution with a more flexible commercially available tagging approach, LA-ICP-MS is a better fit where resolution can be partially sacrificed in exchange for increased throughput while maintaining the multiplexing capability[4]. High throughput is extremely useful for certain medical applications where fast analysis of tissue samples is required.

The method includes ablation of the sample by a pulsed laser where ejected matter from a particular spot is moved along with a stream of argon gas. The gas along with the sample is atomized and ionized by plasma produced with the help of an induction coil supplied with alternating radio frequency current[4]. Then the ionized plasma goes through a series of skimmers to achieve the vacuum required by the mass analyzer. Time of flight is one example of a suitable mass analyzer as it has high sensitivity in the required mass range and it is able to simultaneously analyze all tags detected from a single ablation spot. This method allows one to quantify relative concentrations of tagged molecules over the sample surface due to the nearly total ionization of the analyte. As an example, Giesen *et al.* were able to use this method to simultaneously analyze the presence and distribution of three tumor markers on breast cancer tissue[4]. They were able to discern a significantly higher presence of one of them over the other two, something which was not possible to do with conventional tissue staining methods[4]. As mentioned above, the strength of this method lies in its high throughput with only one round of antibody staining and only a single scan required for complete the analysis, however, this comes at the cost of decreased spatial resolution. At present, with current technology available, the spatial resolution of this method is at least 3 times worse than microscopy-based methods and more than an order of magnitude worse than other mass spectrometry methods[4] (refer to Table 1 below for additional details).

2.3.3 NP-SIMS

In the Schweikert lab, a unique mass spectrometry technique was developed which uses nanoparticle projectile impacts as nanoprobes to sample the topmost layer

of the surface to study co-localization of species within a 10-20 nm area. Since each impact is separately detected, it is possible to select ions of interest and to analyze which species co-localize with them. Using NP-SIMS in the event-by-event bombardment detection mode, multiple studies on biological samples were performed investigating lipid composition in mammalian brain tissues,[8,9] characterization of Qβ and M13 bacteriophages[10] and analysis of tagged CD4 protein on model T-cells.[11] The latter one is the most relevant to the present work as it was the first NP-SIMS study to analyze tagged proteins on a cell surface and is discussed in detail below. The study focused on model T-cells which were labeled with anti-CD4 antibodies (Ab) conjugated to Au nanoparticles (AuNP) and then analyzed by NP-SIMS. C_{60} projectiles were used bombarding the sample surface at random and several types of impacts were detected. The different scenarios or events include projectiles impacting the lipid membrane of a cell and Ab-AuNP conjugates[8]. The presence of lipid membrane fragments and Au secondary ions in the same spectrum proves that Ab molecules were indeed residing on the surface of a cell. Other mass spectra did not have lipid fragments and were assumed to originate from Ab-AuNPs deposited onto glass substrate between the cells[8]. By calculating the number of impacts where gold tags on cell surfaces were detected compared to the total impacts on cells, CD4 density on the cell surface was determined. The calculation was confirmed by SEM. It is important to note that this method's strengths lie in analysis and quantification of nano domains and nano objects, such as nanoparticle tags, and their immediate environments because it uses a time-of-flight (ToF) mass analyzer so that data can be collected on all tags present in the

sample simultaneously. A multi-anode detector allows for detection of multiple isobaric ions from each impact if they are present.

2.4 Summary of Techniques Discussed

The advantages and disadvantages of the presented methods are summarized in table 1. Main capabilities are classified relative to each other as “low,” “medium,” or “high.”

Table 2.1 Summary of analysis methods.

Method	**Max Resolution**	**Potential Multiplexing Capability**	**Throughput**	**Imaging Capability**
Classical Approaches	300 nm	medium	medium	yes
Super-Resolution Microscopy	50 nm	low	low	yes
NanoSIMS	33 nm	high	medium	yes
LA-ICP-MS	1000 nm	high	high	yes
NP-SIMS	10 nm[1]	high	medium	no[2]

[1]Resolution with which co-localization can be established.
[2]Mapping with resolution of 1000 nm is possible[12]

2.5 Extracellular Vesicles (EVs)

For proof-of-concept experiments in this dissertation, EVs have been picked as a target of study. EVs are divided into two major classes: exosomes and microvesicles. Microvesicles are directly pinched off the plasma membrane while exosomes are

produced by pinching into specialized endosomal structures inside the cell. EV membrane mainly consists of a lipid bilayer with embedded proteins. Exosome membranes are enhanced up to a hundred times in certain proteins, such as tetraspanins like CD9, CD63 and CD81, which can be used as markers to differentiate them from microvesicles[13]. Additionally, microvesicles tend to be slightly larger with 100-1000 nm size distribution while exosomes are generally between 30 and 120 nm in size[13]. EVs are important for cell-to-cell signaling without direct cell-to-cell contact. They have been shown to transport ligands, receptors, lipids and RNA between cells[13]. EVs have been found to play vital roles in mechanisms of a multitude of disease including cancer[13]. The protein and lipid composition of EVs will change depending on the type of the cell shedding them as well as the current state of those cells (e.g. inhibition or activation of certain signaling pathways, stress or disease)[13]. This makes it possible to use EV characterization as a non-invasive diagnostic tool for certain types of diseases including cancer. The challenge with studying EVs, and exosomes in particular, is their small size (<120 nm) thus requiring techniques with nanometric resolution (examples of which have been described above).

2.6 References

(1) A. McCabe, M. Dolled-Filhart, R. L. Camp, and D. L. Rimm, J. Natl. Cancer Inst. **97**, 1808 (2005).

(2) C. Chen, S. Zong, Z. Wang, J. Lu, D. Zhu, Y. Zhang, Y. Cui, ACS Appl. Mater. Interfaces **8**, 25825 (2016).

(3) D. R. Bandura, V. I. Baranov, O. I. Ornatsky, A. Antonov, R. Kinach, X. Lou, S. Pavlov, S. Vorobiev, J. E. Dick, S. D. Tanner, Anal. Chem. **81**, 6813 (2009).

(4) C. Giesen, T. Mairinger, L. Khoury, L. Waentig, N. Jakubowski, U. Panne, Anal. Chem. **83**, 8177 (2011).

(5) X. Lou, G. Zhang, I. Herrera, R. Kinach, O. Ornatsky, V. Baranov, M. Nitz, M. A. Winnik, Chem., Int. Ed. **46**, 6111 (2007).

(6) C. Lechene, F. Hillion, G. McMahon, D. Benson, A. M. Kleinfeld, J. P. Kampf, D. Distel, Y. Luyten, J. Bonventre, D. Hentschel, K. M. Park, S. Ito, M. Schwartz, G. Benichou, G. Slodzian, Journal of Biology **5**, 20 (2006).

(7) M. Angelo, S. C. Bendall, R. Finck, M. B. Hale, C. Hitzman, A. D. Borowsky, R. M. Levenson, J. B. Lowe, S. D. Liu, S. Zhao, Y. Natkunam, G. P. Nolan, Nature Medicine **20**, 436 (2014).

(8) F. A. Fernandez-Lima, J. Post, J. D. DeBord, M. J. Eller, S. V. Verkhoturov, S. Della-Negra, A. S. Woods, E. A. Schweikert, Anal. Chem. **83**, 8448 (2011).

(9) F. A. Fernandez-Lima, J. D. DeBord, E. A. Schweikert, S. Della-Negra, K. A. Kellersberger, M. Smotherman, Surf. Interface Anal. **45**, 294 (2013).

(10) C.-K. Liang, S. V. Verkhoturov, Y. Bisrat, S. Dikler, J. D. Debord, F. A. Fernandez-Lima, E. A. Schweikert, S. Della-Negra, Surf. Interface Anal. **45**, 329 (2013).

(11) L.-J. Chen, S. S. Shah, J. Silangcruz, M. J. Eller, S. V. Verkhoturov, A. Revzin, E. A. Schweikert, International journal of mass spectrometry **303**, 97 (2011).

(12) M. J. Eller, S. V. Verkhoturov, S. Della-Negra, and E. A. Schweikert, Review of Scientific Instruments **84**, 103706 (2013).

(13) G. Van Niel, G. d'Angelo, G. Raposo, Nature Reviews Molecular Cell Biology **19**, 213 (2018).

3. EXPERIMENTAL

3.1 Tagging

As mentioned earlier, to detect proteins with NP-SIMS, they must be tagged. Four types of tags were considered and tested during this study: chelated polymer scaffold tags (Maxpar, South San Francisco, CA), metal nanoparticle (NP) tags, halide-containing small molecule tags and lanthanide-chelated BHHTEGST tags. It should be noted that BHHTEGST is also one of the 3 halide-containing small molecule tags used. Chelated polymer scaffold tags contain a lanthanide metal chelated onto a X8 polymer scaffold which is in turn conjugated to Ab of interest via maleimide chemistry. Au NP tags (Cytodiagnostics, Burlington, Ontario, Canada) used in the study have a metal core ~5 nm in diameter capped by 5kDa PEG which makes them soluble in aqueous solutions as well as allowing their conjugation to Ab of interest via NHS chemistry. Halide-containing small molecule tags used in this study were BHHTEGST (fluoride tag), eosin (bromide tag; MarkerGene Tech, Eugene, OR) and erythrosine (iodide tag; EMP Biotech, Berlin, Germany). BHHTEGST was synthesized from the commercially available BHHCT (AdipoGen, San Diego, CA) in order to increase the tag's hydrophilicity so that more of the them can be conjugated to the Ab of interest. Loading the Ab with more tag molecules improved the yield of characteristic ions (by 3 times in case of BHHTEGST). BHHTEGST synthesis was performed by Jesse Sandoval according to the method[1] developed by Sayyadi *et al.* with support of the Bergbreiter lab (detailed procedure in appendix A). Reactive groups used to conjugate them to Ab were NHS for BHHTEGST and eosin and isothiocyanate for eosin. What all four tagging approaches had in common was that they would be conjugated to an antibody (Ab)

which would in turn bind to a protein of interest on the sample surface. Details of the tagging procedures are described in the Appendix A. Comparison of the tagging approaches is given in Table 3.1.

Table 3.1 Comparison of tagging approaches used in the study.

Tagging Approach	Tag Moeity Used in the Study	Pros	Cons
Chelated polymer scaffold	^{142}Nd ions	Commercially available Ready for multiplexing Same chemical and physical properties	Low density of tag
Metal nanoparticles	Au ions	Large amount of tag concentrated in small volume (5 nm in diameter)	Surrounded by a >4 nm layer of cap+Ab which shields tag core
Halide-containing small molecules	F, Br, I ions	Tag concentrated on the surface of Ab with high density	Differences in hydrophobicity among the tags Lack of further multiplexing prospects
Lanthanide-chelated BHHTEGST	Eu, Sm ions	Same chemical and physical properties Multiplexing prospects	Require laser post-ionization to be suitable for "real" biological samples

3.2 Model Surface Preparation

Model surfaces were prepared at the Revzin lab (Mayo Clinic) and shipped to the Schweikert lab for analysis (detailed procedures described in appendix A). Brief model surface preparation for each tagging approach is given below. ^{142}Nd chelated polymer scaffold-Ab conjugates were attached, as a sub-single layer, onto a Si wafer functionalized by (3-Aminopropyl)-triethoxysilane (APTES) and glutaraldehyde (GA) via free amine groups. For the Au NP tag, a mouse Ab single layer surface was prepared by attaching the mouse Abs onto sulfo-NHS-functionalized ITO glass slide. The mouse Ab surface was then labeled with Au NP anti-mouse Ab conjugates. BHHTEGST-Ab, eosin-Ab, erythrosine-Ab and Eu/Sm-chelated BHHTEGST-Ab conjugates were covalently attached as a sub-single layer to a functionalized Au-coated Si wafer via sulfo-NHS chemistry.

3.3 Extracellular Vesicles (EVs) Preparation

The model biological sample chosen in this study was urine EVs (an introduction to EVs can be found in the literature review chapter). Surface sample preparation was done by Yong Duk at the Revzin lab (Mayo Clinic) and then shipped to the Schweikert lab for analysis. EVs were isolated from urine donated to the Mayo Clinic by healthy individuals using centrifugation. The EVs were attached to an ITO glass slide functionalized by poly-L-lysine via electrostatic interactions using a microfluidic device and then labeled with erythrosine conjugated to anti-podocin Abs (detailed procedure in appendix A). It is important to note that NP-SIMS requires vacuum compatible samples, however, EVs are vesicles primarily consisting of a lipid bilayer and would rapture under vacuum conditions. In order to make attached EV samples vacuum compatible, they were fixed via crosslinking, dehydrated using critical point drying and preserved on dry ice until analysis by NP-SIMS (detailed procedure in appendix A). The second set of EV samples where CD63 and CD81 were tagged with erythrosine and BHHTEGST respectively were prepared by Bruno Crulhas at the Revzin lab (Mayo Clinic). The only difference in preparation to the first set of EV samples was that they were dehydrated under 10^{-3} Torr vacuum.

3.4 Instrument

Figure 3.1 shows a diagram[2] of the custom NP-SIMS instrument used to analyze the samples in this study. The liquid metal ion source (LMIS)[3] consists of an etched needle with a reservoir containing gold silicon eutectic. The eutectic is 97.15% Au and 2.85% Si. When the eutectic is heated to 363 degrees Celsius, it transitions into a liquid phase and positively charged Au clusters can be extracted from the needle using an electric field (+20 kV). The source assembly is mounted on micro-positioners (X, Y directions)

that can be used to align the needle with ion extraction electrode. The resulting projectiles pass through a Wien filter. The Wien filter consists of perpendicular electric and magnetic fields which selects the charged Au clusters based on their velocity that also corresponds to a certain mass to charge ratio or number of Au atoms in the cluster per charge (n/q). There were two massive Au projectiles used in this study. The first is $(Au_{400})^{4+}$, n/q=100, with kinetic energy of 440 keV, when positive secondary ions detected, and 520 keV, when negative secondary ions detected. The second is $(Au_{2800})^{8+}$, n/q=350, with kinetic energy of 880 keV, when positive secondary ions detected, and 1040 keV, when negative secondary ions detected. After acceleration (+100 kV), the selected projectiles are separated in time and space using a pulser which is run at 10,000 to 30,000 pulses per second. Any projectile outside of the pulse window is deflected away from the correct trajectory onto the target sample. The probability of each pulse window to contain a projectile is 0.1. The selected projectiles impact the target surface one by one termed event-by-event bombardment/detection mode. After a projectile impacts the target surface, secondary ions (SIs), electrons and neutrals are sputtered from a volume of 10-20 nm in diameter and ~10 nm in depth. The resulting SIs are extracted and analyzed with a reflectron TOF mass spectrometer separately for each impact. 10 to 30 SIs are produced on average per impact depending on the projectile selected. The SIs are detected using a pie-shaped 8 anode microchannel plate (MCP) detector in case there are multiple isobaric ions in an event. In the negative mode, when negative species are extracted, sputtered secondary electrons are diverted, using a magnetic prism, onto an MCP detector. The detected electron signal is used as a start signal for the SI detector. The secondary ion mass resolution measured

at full-width-half-max (FWHM) varies with mass range. For the mass range of 0-100 amu, mass resolution is 4000 that decreases to 1000 for the mass range of 500-1000 amu. The instrument is run at 1000-4000 projectile impacts per second collecting up to 50 million of individual mass spectra. Software developed in the Schweikert lab called Surface Analysis and Mapping of Projectile Impacts (SAMPI©)[4] is used to produce and analyze the mass spectra. By summing all of the events SAMPI© produces a conventional mass spectrum. In addition, using the co-emission of SIs from individual impacts, a particular ion(s) can be selected and events only containing that ion sorted out to produce a coincidental mass spectrum. Those ions which are co-localized will be enhanced while those that are not found in the immediate environment will be suppressed.

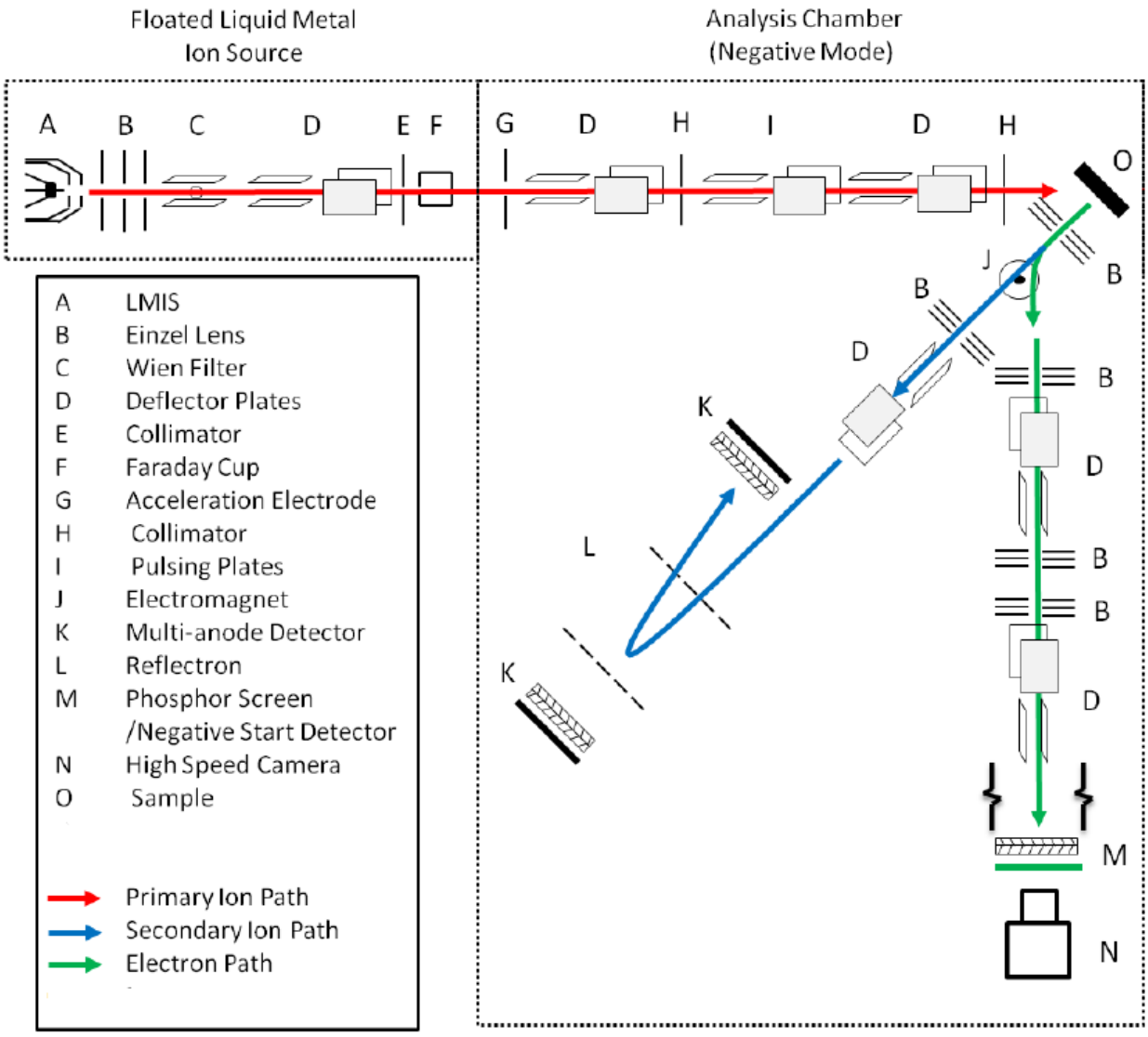

Figure 3.1. Diagram of the custom-built NP-SIMS instrument consisting of a liquid metal ion source (LMIS) and a reflectron TOF mass spectrometer using an 8 anode microchannel plate (MCP) detector. Magnetic prism diverts electrons in negative mode that can be used as a start signal. Reprinted from (Debord, 2012).

3.5 More Efficient Larger Projectile $(Au_{2800})^{8+}$

To improve sensitivity of tag signal, $(Au_{2800})^{8+}$ nano-projectile was developed at the Schweikert lab.[5] This projectile demonstrates ion yield enhancement 2-3 times compared to $(Au_{400})^{4+}$ projectile.[5] The enhancement effect is due to the larger volume sputtered by the $(Au_{2800})^{8+}$ projectile. Determination the size and charge of $(Au_{2800})^{8+}$ nano-projectile was done via neutron activation analysis.[5] Specifically, the size for this projectile is an average value for the experimental mass window distribution shown in figure 3.2.[5] Experiments with neat vapor deposited samples found that molecular ion yields were more than double than with the $(Au_{400})^{4+}$ projectile.[5] The larger sputter volume of 20x20x10 nm^3 for the $(Au_{2800})^{8+}$ projectile allows the detection of tags from 3 co-localized conjugated Abs. As the trade-off for increased sensitivity and signal with the large projectile, the sampled surface area of each impact is increased to at least 20 nm in diameter on average as opposed to 10 nm with $(Au_{400})^{4+}$. Figure 3.3 compares TEM images of impacts by each respective projectile on 10 nm amorphous carbon film.[5]

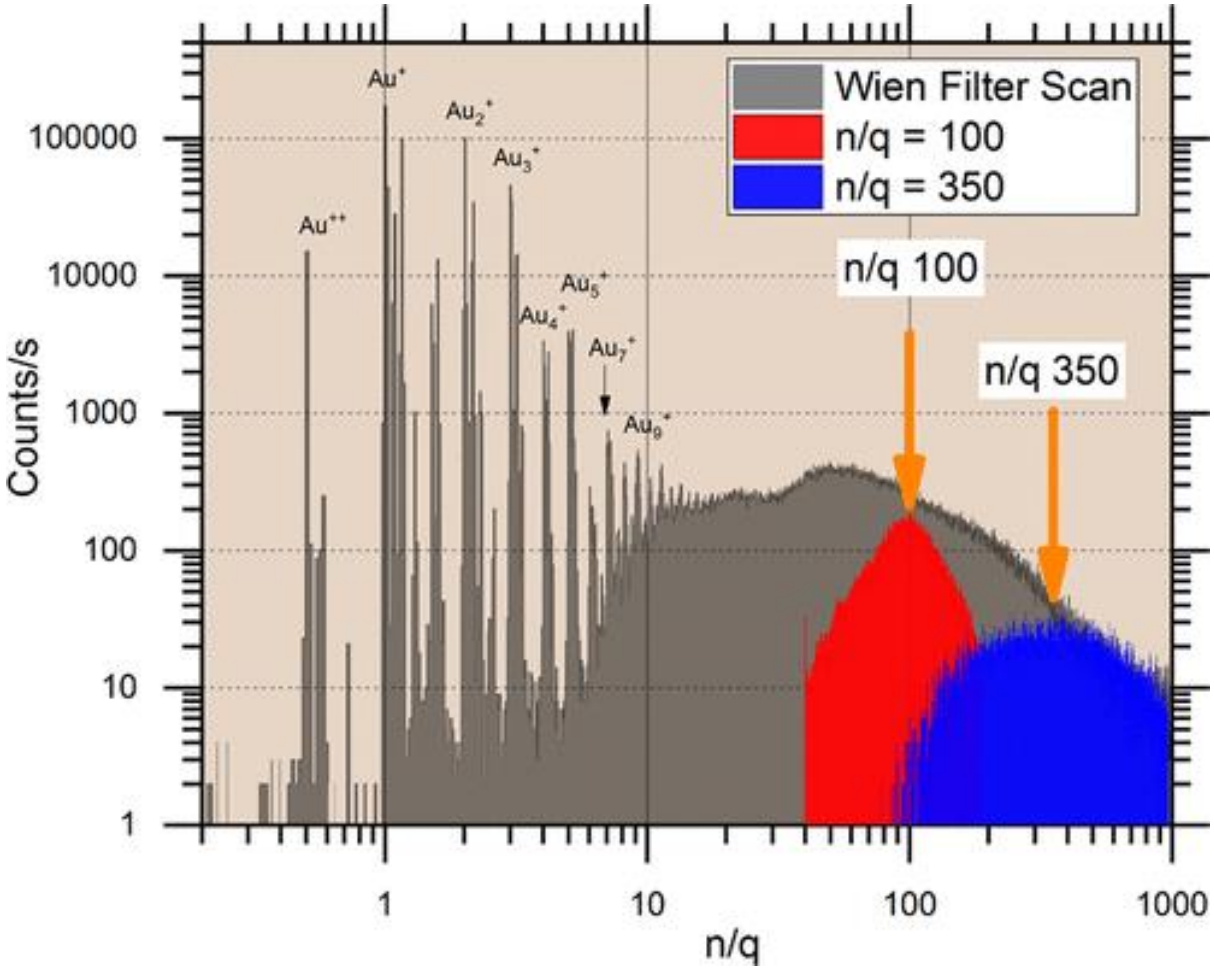

Figure 3.2. Wien filter scan of the possible projectiles produced by the liquid metal ion source as well as representative time-of-flight measurements of n/q=100 or $(Au_{400})^{4+}$ and n/q=350 or $(Au_{2800})^{8+}$. Reprinted with permission from (Eller, 2018). Copyright (2018) American Chemical Society.

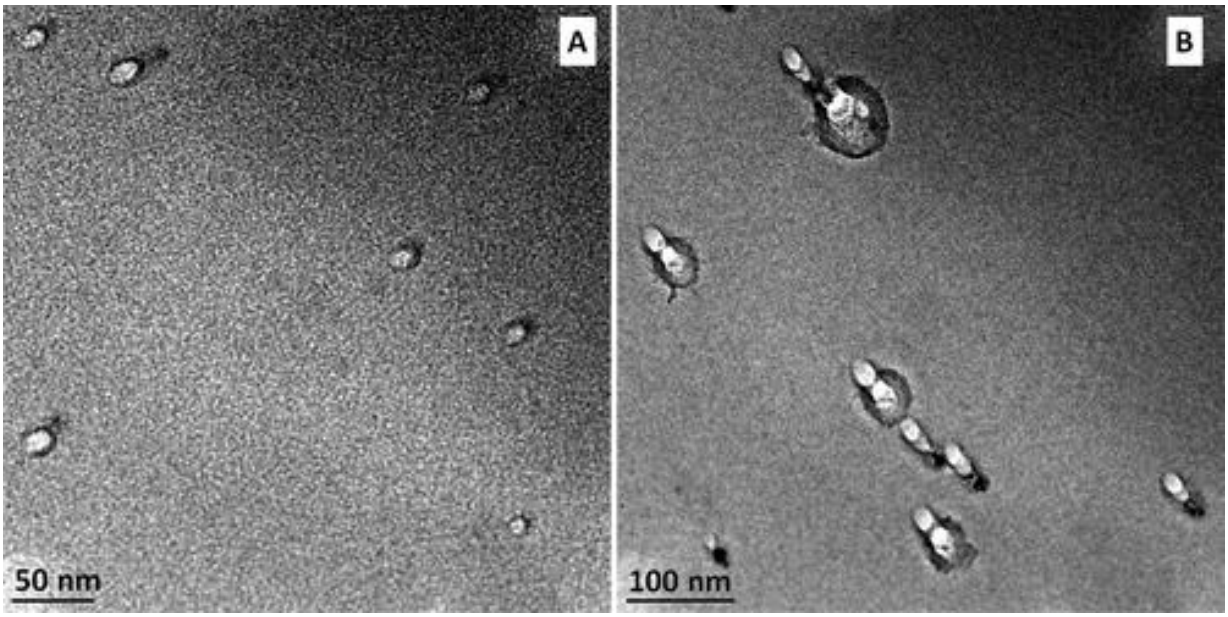

Figure 3.3. Transmission electron micrographs of impact craters on 10 nm amorphous carbon. (A) Impacts of 520 keV Au_{400}^{4+} with a 45° impact angle, scale bar 50 nm. (B) Impacts of 1040 keV Au_{2800}^{8+} with a 45° impact angle, scale bar 100 nm. Reprinted with permission from (Eller, 2018). Copyright (2018) American Chemical Society.

3.6 Beam Tuning, Data Acquisition and Analysis

Initially, once the source starts emission of gold clusters and ions, the beam current is measured by a Faraday cup located at the end of the high voltage platform which can be manually adjusted into the beam path. First, the beam direction is optimized. It is tuned by measuring the Au^+ current (selected using the Wien filter) on the Faraday cup and adjusting the XY position of the source at 30 μA extraction current using the micro-positioners that the source is mounted on and the ion lens which is mounted after the projectile extraction electrode. Once the direction is adjusted, the beam is characterized by checking if the Au^{2+}, Au^+, Au_2^+ and Au_3^+ ion current maxima are at the proper positions in reference to the Wien filter selection. Once the beam direction is tuned and the beam characterized, the extraction current is increased to 55 μA for Au_{400}^{4+} projectile and 100 μA for the Au_{2800}^{8+} projectile. Then the ion lens is tuned to optimize the beam direction and focus.

Next, the time-of-flight (ToF) mass spectrum of the Wien filter-selected beam is measured via bombardment of a reference sample (typically a vapor deposited glycine on a a doped Si wafer). For measurement of this mass spectrum, the start signal is produced by pulser and the stop signal generated by detection of secondary electrons emitted from reference sample. The appropriate ToF for the large projectiles is extrapolated from the known ToF of well-defined smaller projectiles such as Au^{2+}, Au^+, Au_2^+ and Au_3^+. Average ToF of Au_{400}^{4+} is centered at ~90 000 channels of the time-to-digital converter (TDC) (each channel is 120 ps wide) while for Au_{2800}^{8+} the average is at ~160 000 channels of the TDC. The beam direction is then adjusted using three sets of deflectors through two sets of apertures with the second set having the diameters of

500 and 250 µm. An additional time filter is adjusted by gating electronics. As noted earlier, data is acquired using custom acquisition software and then analyzed with custom data analysis software, SAMPI©.[6]

Using co-emission of ions from single impacts, it is possible to quantify the surface coverage area of a specific moiety such as a tag. From the total number of impacts on the sample, N_0, there is a specific set of impacts, N^*, that impacted the tag of interest. Considering the equivalency of impacts,[7] one can calculate the percentage of the probed area where the tag is present, *k*, by taking their ratio.

$$k\ (100\%) = \frac{N^*}{N_0} 100\% \qquad (3.1)$$

To calculate N^*, one can use the correlation coefficient, K^*, of co-emission of ions A and B specific to the tag:

$$K^* = \frac{Y^*_{A,B}}{Y^*_A Y^*_B} \qquad (3.2)$$

where Y^*_A and Y^*_B are the yields (number of emitted ions which are detected per projectile impact) of ions A and B respectively and $Y^*_{A,B}$ is the yield of co-emitted A and B ions. Considering equivalency of impacts and independent emission of ions from each impact, $K^*=1$. The measured yields are given by

$$Y^*_A = I_A / N^* \qquad (3.3)$$

$$Y^*_B = I_B / N^* \qquad (3.4)$$

$$Y^*_{A,B} = I_{A,B} / N^* \qquad (3.5)$$

where I_A is the number of detected A ions, I_B is the number of detected B ions, $I_{A,B}$, is the number of detected co-emitted ions and N^* is the number of impacts on the area of the tag.

Using the expressions (3.2-3.5), one can obtain N^*:

$$N^* = \frac{I_A I_B}{I_{A,B}} \qquad (3.6)$$

Therefore, one can calculate the coverage area of the tag directly from the experimentally measured ion intensities.

3.7 References

(1) N. Sayyadi, R. E. Connally, and A. Tryb, Chem. Commun. **52**, 1154 (2016).

(2) J. D. Debord (2012). Evaluation of Hypervelocity Gold Nanoparticles for Nanovolume Surface Mass Spectrometry. Doctoral dissertation, Texas A&M University. Available electronically from http://hdl.handle.net/1969.1/148083.

(3) M. Benguerba, A. Brunelle, S. Della-Negra, J. Depauw, H. Joret, Y. Le Beyec, M. G. Blain, E. A. Schweikert, G. Ben Assayag, P. Sudraud, Nuclear Instruments and Methods in Physics Research Section B: Beam Interactions with Materials and Atoms **62**, 8 (1991).

(4) M. J. Eller, S. V. Verkhoturov, S. Della-Negra, and E. A. Schweikert, Rev. Sci. Instrum. **84**, 103706 (2013).

(5) M. J. Eller, A. Vinjamuri, B. E. Tomlin, E. A. Schweikert, Anal. Chem. **90**, 12692 (2018).

(6) M. J. Eller (2012). Surface mapping based on the correlated emission of ions and electrons from hypervelocity C60 impacts. Doctoral dissertation, Texas A&M University. Available electronically from http://hdl.handle.net/1969.1/148366.

(7) R. D. Rickman, S. V. Verkhoturov, E. S. Parilis, and E. A. Schweikert, Phys. Rev. Lett. **92**, 047601 (2004).

4. EVALUATION OF TAGS FOR NP-SIMS

4.1 Chelated Polymer Scaffold Tags

4.1.1 Experimental Design

In the literature review chapter, a mass cytometry method was discussed where commercially available lanthanide tags (Maxpar, South San Francisco, CA) were used as mass tags in conjunction with ICPMS. These tags use a polymer scaffold to chelate isotopes of lanthanide metals which are then conjugated to the antibody that binds to the protein of interest. This commercially available tagging approach was tested for compatibility with the event-by event NP-SIMS method.

In order to assess the feasibility of using the Maxpar tags, a model experiment was designed and performed. ^{142}Nd metal ion tags were loaded onto X8 polymers (Maxpar©) via pentetic acid. The polymers contain maleimide caps that bind free sulfhydryl groups on the antibodies (Figure 4.1). Each antibody is conjugated to ~3-4 polymer chains containing ~22 Ln ions. Thus, each antibody is tagged with ~80 Ln ions in total.

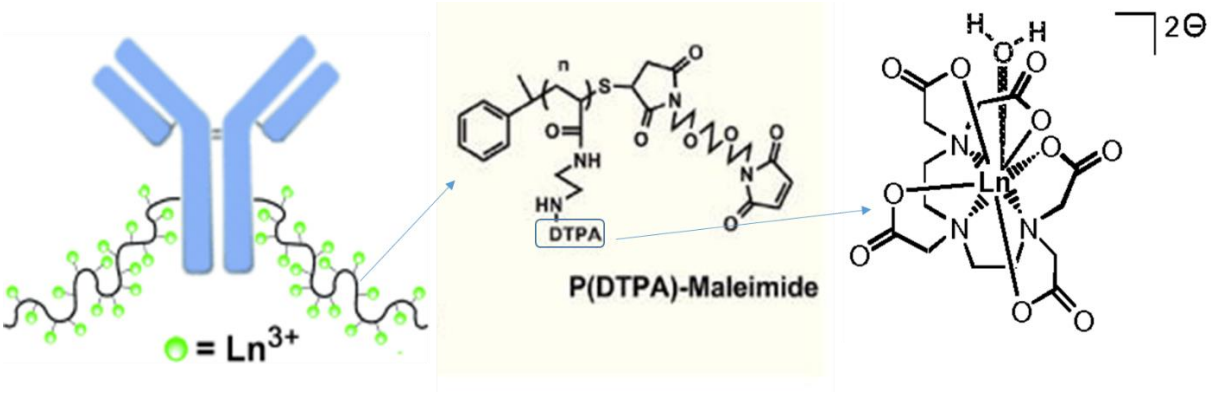

Figure 4.1. Maxpar isotopic metal tag conjugation.

Next, in order to approximate a membrane surface, the conjugates were attached as a sub-single layer onto the surface of a silicon wafer. Specifically, the Si wafer was functionalized by (3-Aminopropyl)-triethoxysilane (APTES) and glutaraldehyde (GA) as shown in figure 4.2. Then the free amine groups on the tagged conjugates reacted with the GA groups to form the topmost layer of the sample. Sequential samples were prepared at each stage of the model sample preparation process so that proper functionalization and subsequent attachment of the tag-conjugated Abs can be confirmed and analyzed. There were 3 samples in total: sample 1 consisted of the APTES/GA functionalized Si wafer, sample 2 included an antibody layer on the surface bound to the functionalized APTES/GA Si wafer and sample 3 had ^{142}Nd conjugated-Ab attached to the APTES/GA Si wafer.

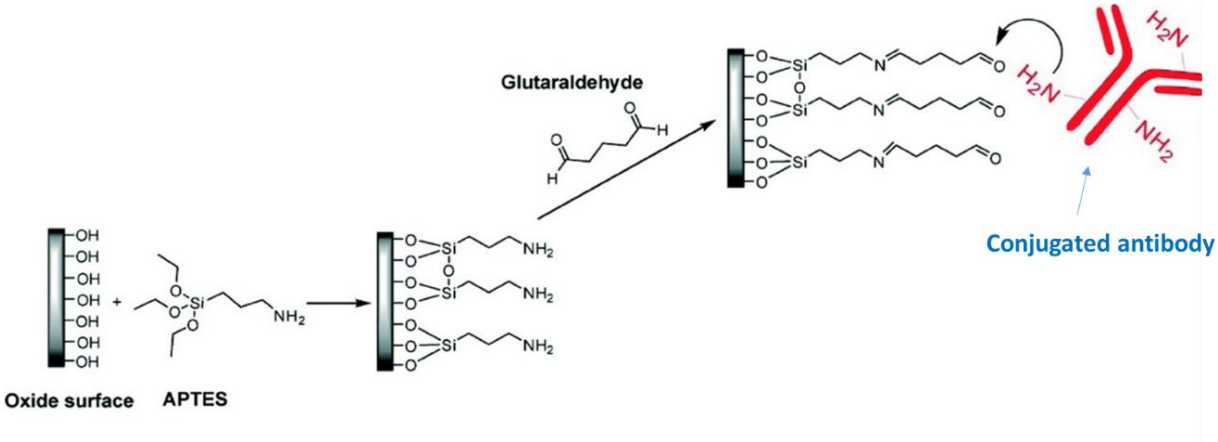

Figure 4.2. Functionalization of Si wafer and attachment of conjugated antibodies for the model experiment.

4.1.2 Results

The mass spectra obtained after analysis by Event-by-Event NP-SIMS for each of the three samples are shown in figures 4.3 to 4.6 below. The coverage calculations shown were done according the method described in the experimental chapter. As seen in figures 4.3 to 4.5, the APTES/GA functionalization was successful with 80%, 90% and 75% surface coverage for sample 1, 2 and 3 respectively; however, the surface was not completely functionalized. The Abs and Ab conjugates attached as a sub-single layer with only 8% and 9% surface coverage in the sampled area for samples 2 and 3 respectively. It is important to note that the conjugation of Abs to the ^{142}Nd-chelated polymer scaffold did not affect the efficiency of their attachment to the APTES/GA surface. Using positive mode (figure 4.6), where we detect positive SI ions, we were able to detect ions coming exclusively from the tag ($^{142}Nd^{+}$ and $^{142}NdO^{+}$). Using these ions, we calculated the surface coverage by the Nd tag and it matched the coverage by Ab that was calculated from the negative mode spectrum confirming near complete labeling of antibody by Nd tag as per Maxpar© kit specifications.

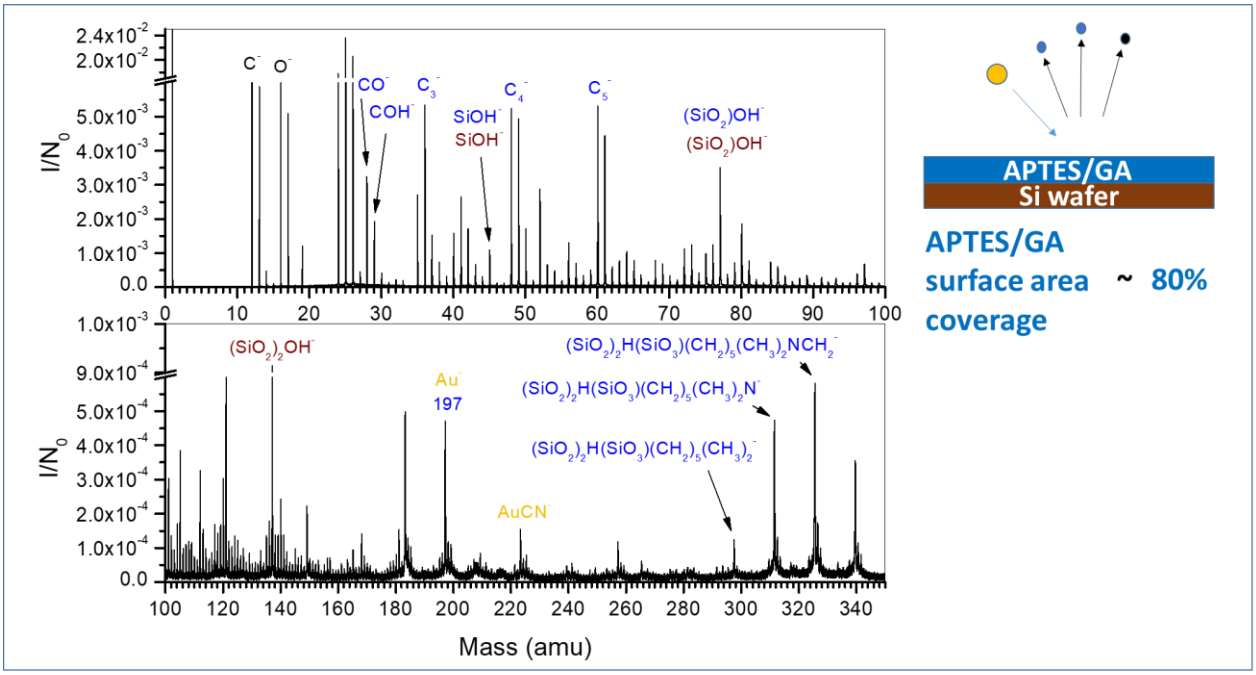

Figure 4.3. Negative ion mass spectrum of APTES/GA functionalized Si wafer (Sample 1) using 520 keV Au_{400}^{4+} projectiles.

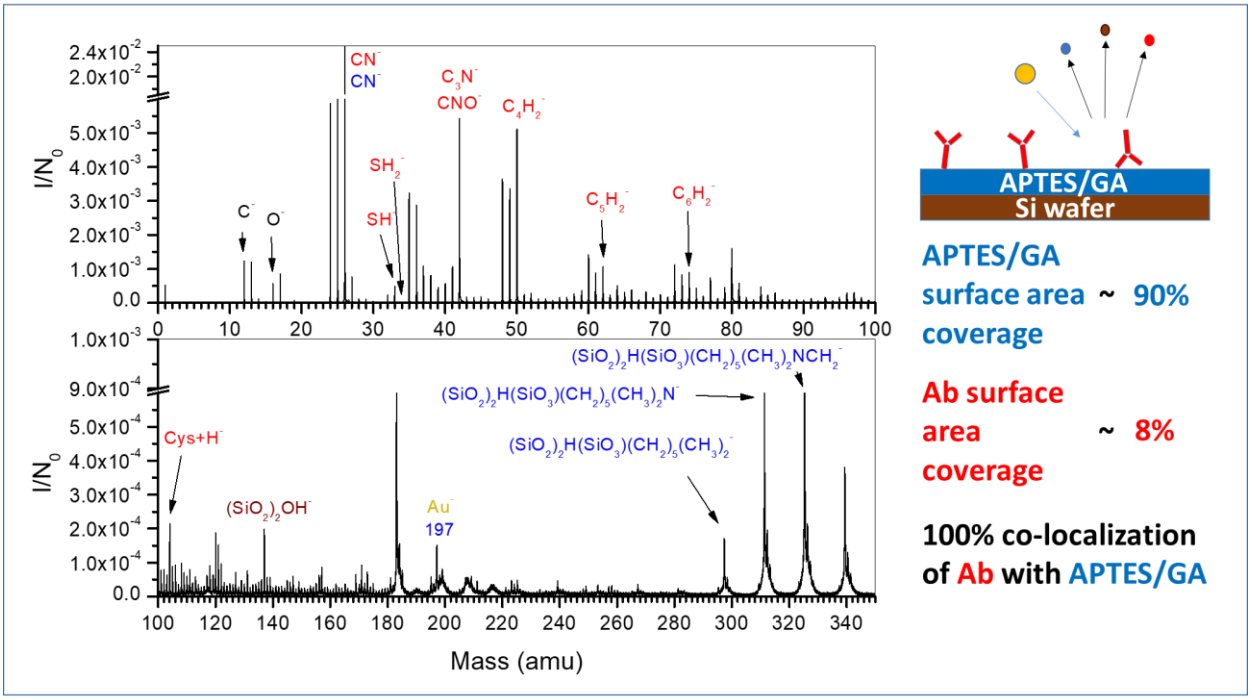

Figure 4.4. Negative ion mass spectrum of APTES/GA functionalized Si wafer with attached antibody (Ab) (Sample 2) using 520 keV Au_{400}^{4+} projectiles.

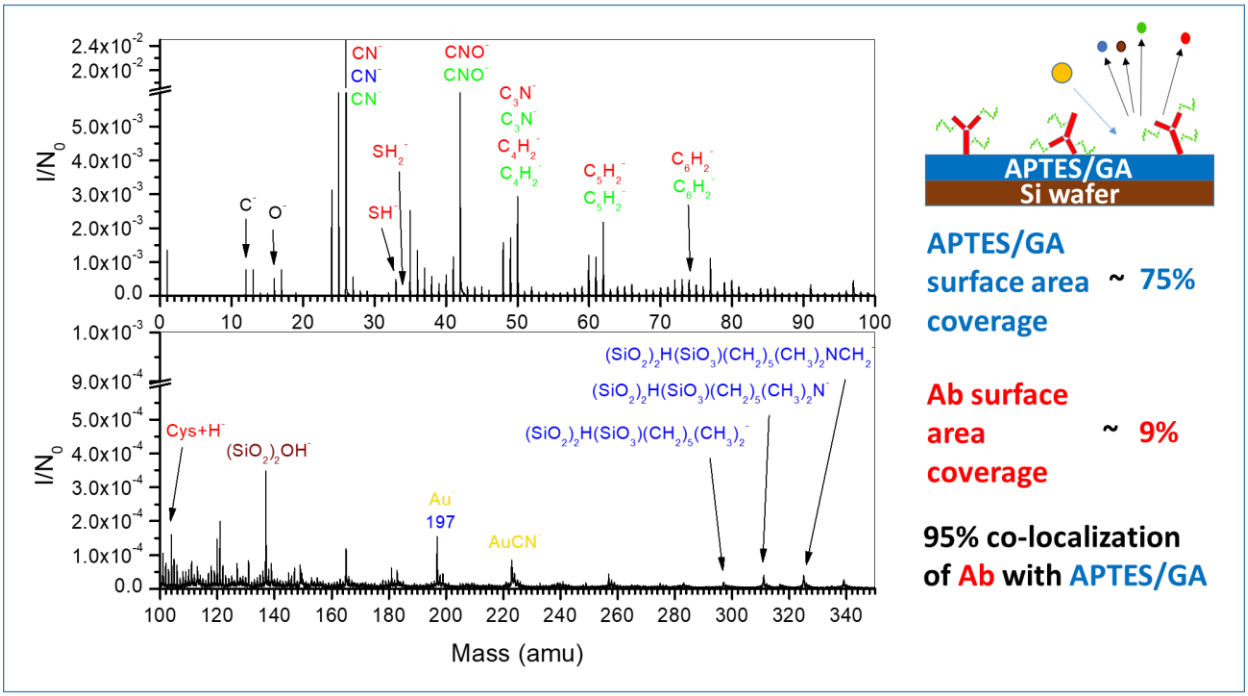

Figure 4.5. Negative ion mass spectrum of APTES/GA functionalized Si wafer with attached antibody (Ab) conjugated to Nd/polymer tag (Sample 3) taken using negative mode and 520 keV Au_{400}^{4+} projectiles.

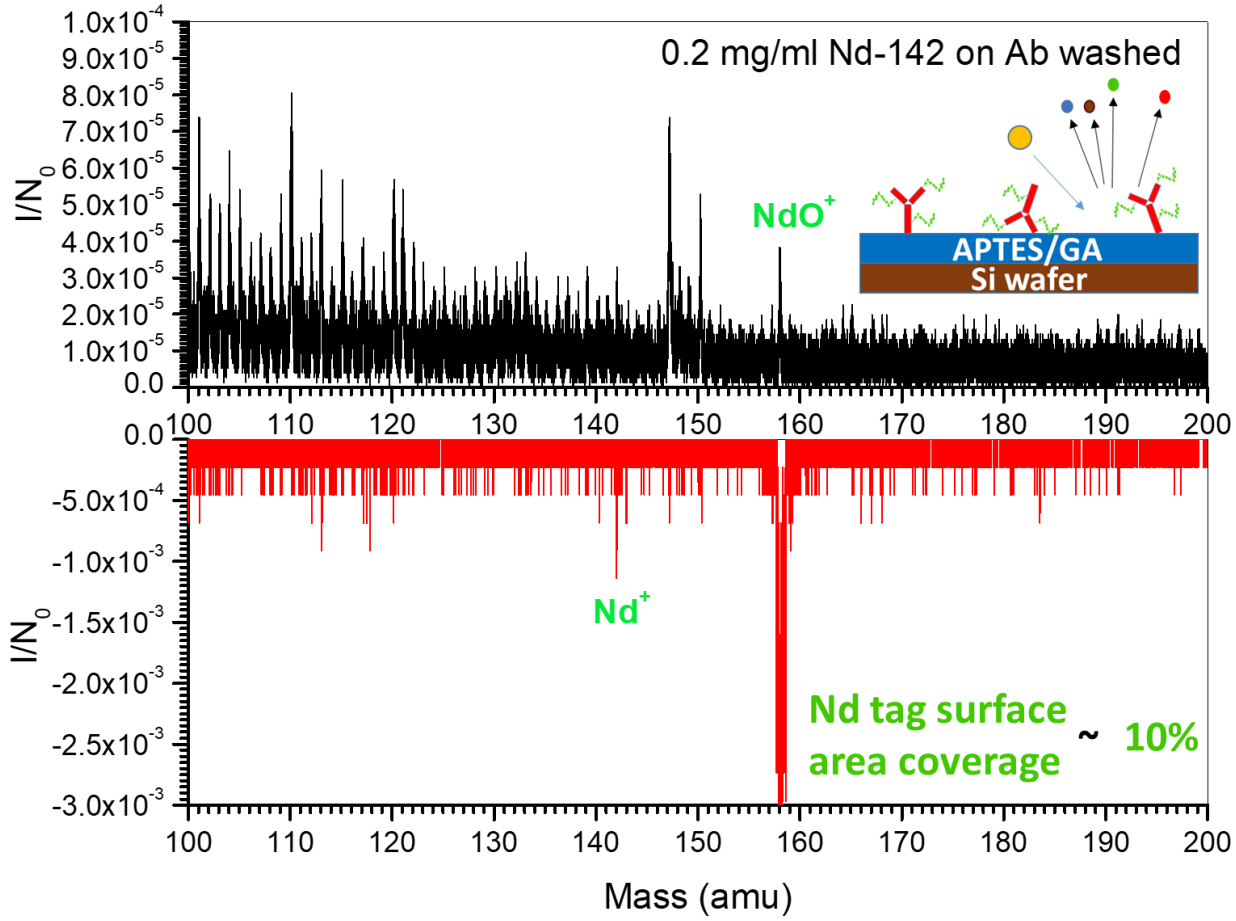

Figure 4.6. a) Positive mode total mass spectrum taken using 440 keV Au_{400}^{4+} projectiles showing the NdO^+ peak. b) Mass spectrum showing co-emission with NdO. Nd tag antibody conjugate coverage was 10%.

The antibody and APTES/GA functionalization co-localized with each other indicating that the attachment was successful and according to the experimental design. Surface area coverage of the isotopic metal tag was found to be ~10% using the methodology described in the experimental chapter. Based on the approximate tagged antibody size and the calculated coverage, the surface density of the tagged antibodies was ~540 molecules per μm^2 in the probed area of 250 µm in diameter. Therefore, a reference-free approach to localized surface quantification was demonstrated.

4.1.3 Conclusions

Even though the tag was successfully detected and quantified using the event-by-event NP-SIMS approach in a model experiment, the signal from the Nd tag chelated to the X8 polymer scaffold was not strong enough to use with real biological samples such as cells or EVs. The expected concentration of proteins of interest on either cells or EVs in the sampled area is expected to be one to two orders of magnitude less than what we had for the model target described above. Therefore, even in the best-case scenario, the Nd tag signal would not meet the acceptable limit of detection threshold of three times above background.

4.2 NP Tagging Approach

4.2.1 Experimental Design

In an attempt to improve the tag signal, metal/metal oxide nanoparticle (NP) tags were tested. A metal nanoparticle of 5 nm in diameter has ~6000 metal tag atoms in a similar volume as the polymer scaffold tags described above of ~65 nm^3. The concept is illustrated in fig 4.7.

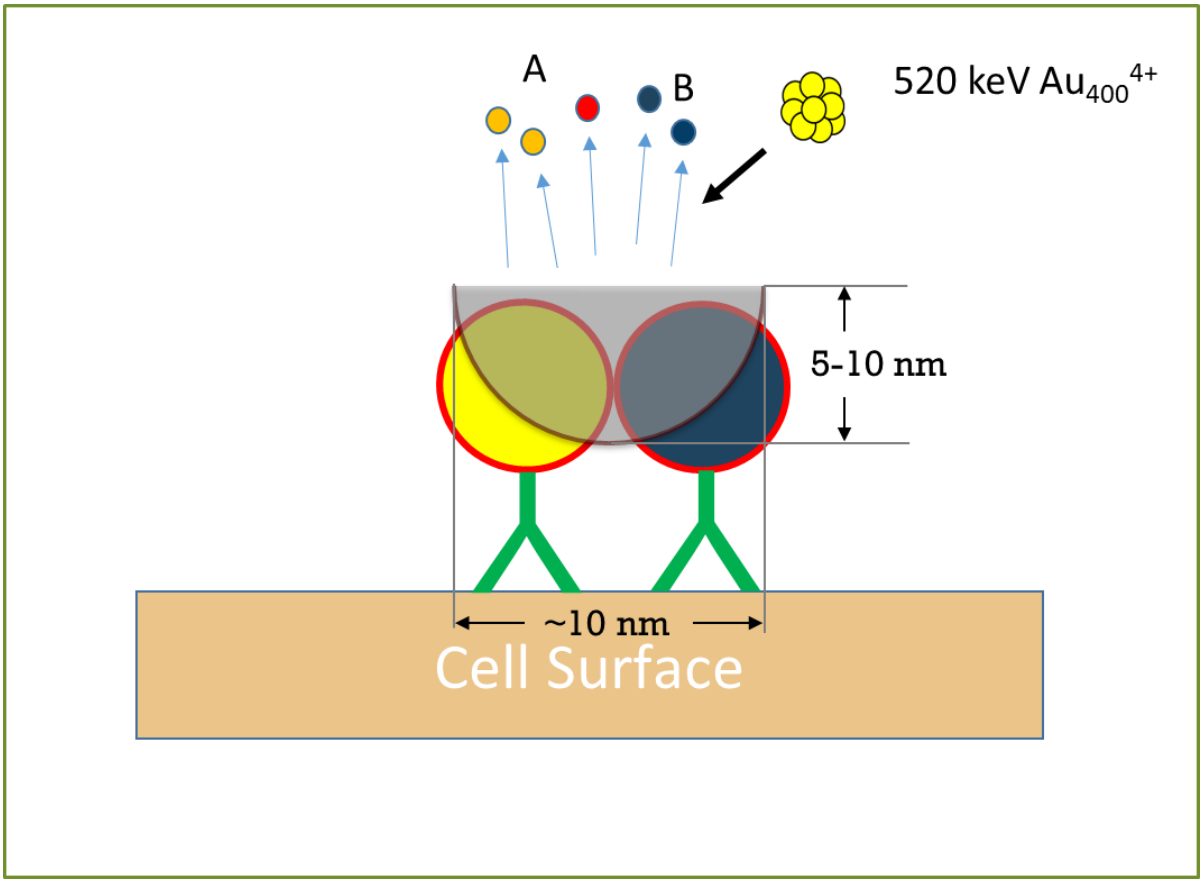

Figure 4.7. Experimental concept of using NP tags with NP-SIMS method.

Au nanoparticles of 5 nm in diameter were used in a model experiment to test the feasibility of NPs as protein tags for NP-SIMS. The Au NPs were coated with PEG layer of 4 nm that had a terminal NHS group that could be conjugated to antibody of interest. The experimental design for the model NP experiment is shown in fig 4.8. Briefly, the 5 nm AuNPs were conjugated to anti-mouse Abs. Then a functionalized ITO surface was prepared onto which mouse Abs were bound in a single layer. The mouse Ab surface was then labeled with AuNP-Ab conjugates and analyzed with NP-SIMS.

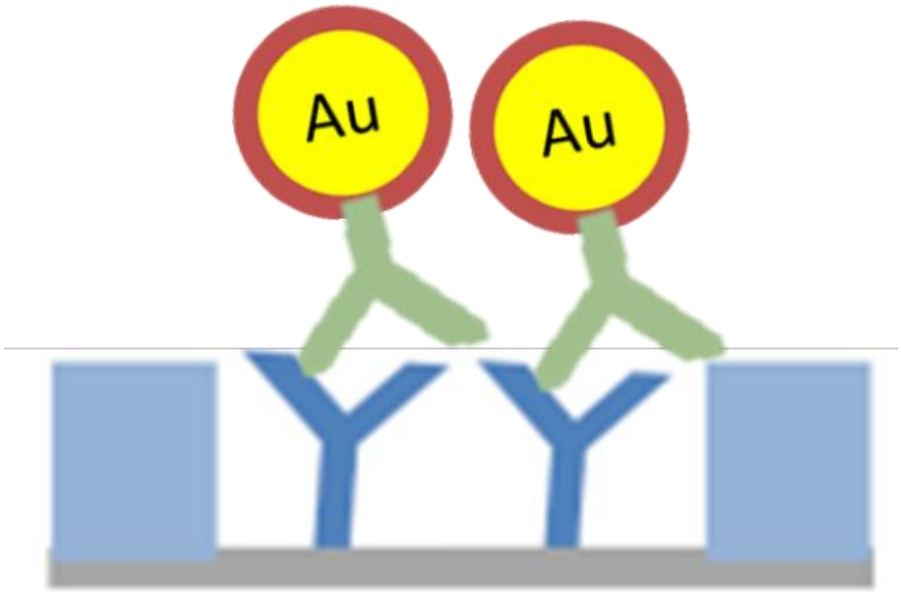

Figure 4.8. Model experimental design for AuNP-Ab tagging. ITO glass was functionalized by mouse antibodies inside of a PDMS well and then tagged by AuNPs to model cell surface conditions.

4.2.2 Results

The resulting mass spectrum is shown in figure 4.9a. A control mass spectrum shown in figure 4.9b was taken from a spot outside the PDMS well. As seen in the mass spectrum in figure 4.9a, ions related to AuNPs were detected from the area inside the PDMS well, while outside the well, there is strong signal from ITO related ions such as $In_3O_2^-$ and $In_3O_3^-$ (figure 4.9b). By calculating the surface area covered by AuNP tags and dividing by the known average cross-sectional area of the AuNP, the surface density of the tags was found to be 9.6×10^3 AuNPs/μm^2 which falls in the middle of the theoretical limits for the number of antibodies on the surface (between 4.4×10^3 and 1.3×10^4 Abs/ μm^2 depending on their packing).

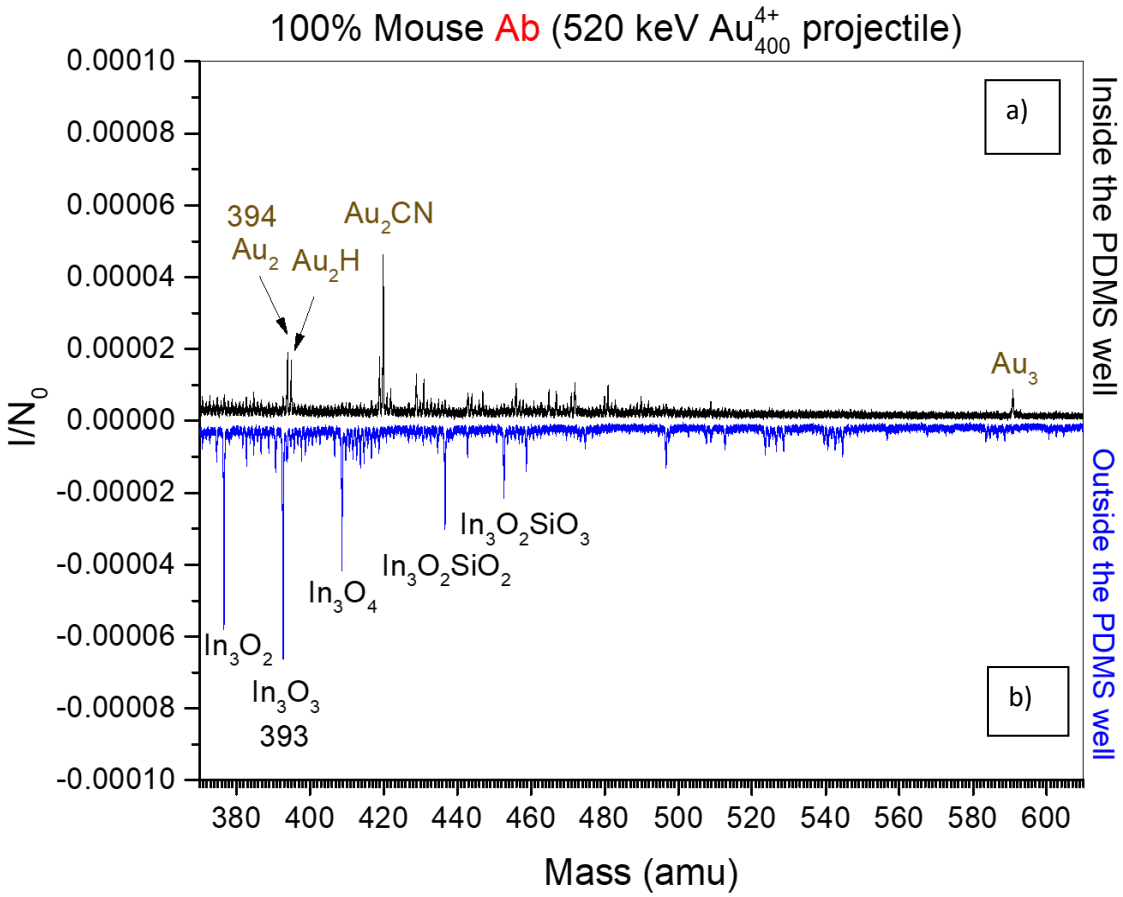

Figure 4.9a,b. Mass spectra of AuNPs conjugated to mouse Ab. a) Area of the sample where AuNP-Ab were deposited (inside the PDMS well). b) An area of the sample outside the PDMS well.

4.2.3 Conclusions

Using 5 nm AuNP tags, we were able to detect the conjugated Abs on a model single layer surface. Furthermore, the signal was improved by an order of magnitude when compared to the chelated polymer scaffold tagging approach. However, when other metal NPs were tested such as 5 nm Ag and iron oxide (FeO) nanoparticles, the signal was again not sufficient for use with “real” biological samples.

The question is, why is the signal so low despite the NPs containing ~6000 tag atoms? There are two main issues in that regard as illustrated in figure 4.10, the thickness of the NP cap and the amount Abs attached on their surface. It is important to remember that NP-SIMS is only able to probe up to 10 nm in depth, however, the thickness of the NP cap is at least 4 nm (that was the thinnest cap among commercially available NPs). In addition, on top of the cap, there is also a layer of conjugated Abs. Together the two layers above the NP metal core inhibit emission of Au ions to the point that it is no longer usable with “real” biological samples. Another issue is that the large number of Abs increases the overall size of the tag so that it is difficult to effectively probe two co-localized tagged species on the surface with a single projectile impact. Experiments were performed to sort out NP-Ab conjugates with fewer Abs bound on the surface using chromatography, however, the success was limited (data not shown).

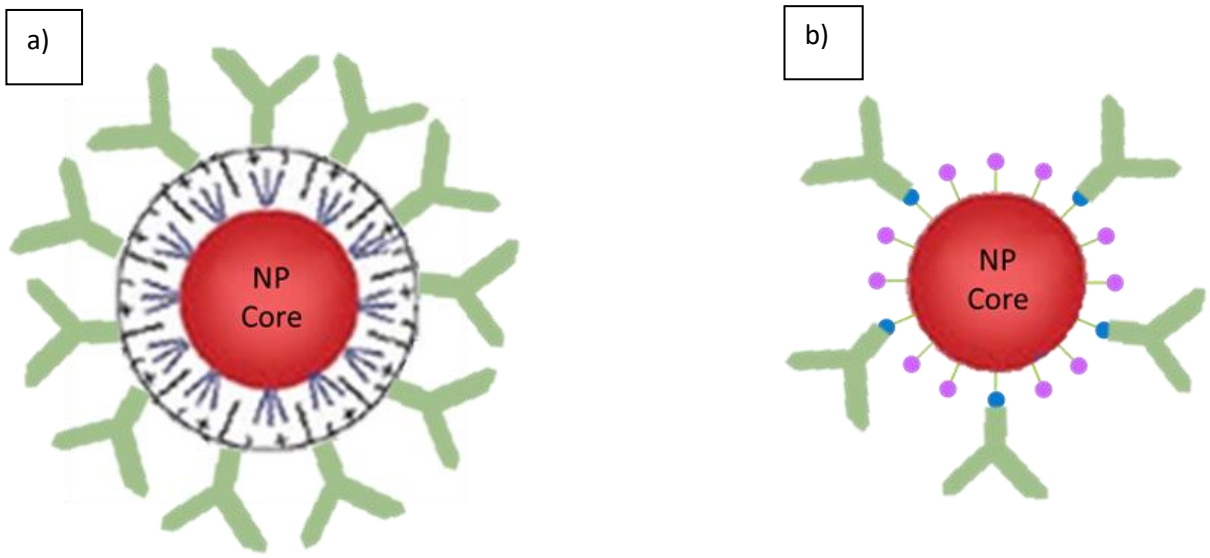

Figure 4.10a,b. a) Illustration of the NP-Ab conjugates which were prepared. b) Depiction of how the NP-Ab conjugate can be improved to increase signal from the tag with a thinner cap and fewer attached Abs.

An alternative tagging approach was pursued where Abs of interest are conjugated with molecular tags such as BHHTEGST, eosin and erythrosine. The resulting conjugates are limited to a single Ab in size and are more compact than the (chelated polymer scaffold)-Ab conjugates, solving the issues encountered with the above tagging approaches. This approach was used for the subsequent experiments described in the following chapters.

5. ULTRA-SENSITIVE DETECTION OF TAGGED PROTEINS IN VESICLE MEMBRANES WITH NANO-PROJECTILE SECONDARY ION MASS SPECTROMETRY

(Expanded from a manuscript to be submitted to Biointerphases:

D. S. Verkhoturov[1], M. J. Eller[1], Y. D. Han[2], B. Crulhas[2], S. V. Verkhoturov[1], A. Revzin[2], E. A. Schweikert[1]

[1]Department of Chemistry, Texas A&M University, College Station, TX 77843, USA;

[2]Mayo Clinic, 200 1st Street SW St-11-14, Rochester, MN 55905, USA)

5.1 Introduction

One of the current challenges in spatially resolved bio-analysis, is the characterization of cellular surfaces at the nanoscale. The task is daunting given the range of molecules of potential interest, and is compounded by detection constrained to a nano-volume. The methodologies pursued aim for ultra-sensitive detection of analytes by targeting them with selective binding agents, each tagged with a specified fluorophore or an unusual isotope.[1,2,3] Tagged moieties can then be localized in extremely small numbers, down to single molecules, with super-resolution microscopy techniques.[4] Their space of application is delineated by tagging requirements and the characteristics of the fluorophores.[4] Another versatile approach for nano-volume assays relies on secondary ion mass spectrometry, SIMS, with highly focused primary ion probe beams.[3,5] Characterization of isotopically-tagged moieties in surface layers with a spatial resolution of 50-200 nm (Nano-SIMS) has been reported.[3,5,6,7,8] For example, by incorporating isotopically labeled sphingolipids, Nano-SIMS was able to show the

presence of sphingolipid nano-domains, likely to be lipid rafts, in the plasma membrane of intact mouse fibroblast cells.[8] In addition to isotopic tagging, uncommon element tagging and immunolabeling of lipids and proteins that participate in formation of membrane nano-domains has been applied to Nano-SIMS studies.[9,10] We discuss below the performance of nano-projectile SIMS, NP-SIMS, which enables detection of molecules within ~20 nm. NP-SIMS has been described previously.[11] Briefly, a surface is probed with a sequence of energetic individual gold nanoparticles (1040 keV Au_{2800}^{8+}), each separated in time and space. The incident nanoparticle acts as a nanoprobe, causing emission of secondary ions, SIs, from ~20 nm. Depth of emission is ~10 nm, hence well suited for membrane analysis. Multiple SIs are ejected from a single impact.[12] However, it is in most cases not possible to validate the identity of an analyte at that level. The concept is to probe the surface layer stochastically on a few million nanospots, one-by-one, and to record the emissions from each site separately. The data from the collection of impacts will contain information of like-sites. They can be grouped for accurate identification of analytes and evaluating correlations among co-emitted species.[12,13] The latter in turn reveal molecular environments, e.g. nanoscale homogeneity, ligand loading on nanoparticles, the identity of nanometric inclusions, dispersion of catalytically active moieties.[14,15,16,17,18] It is important to note that tagging is a prerequisite for the applications in SIMS as the size of the ejecta generated by atomic ion, cluster of particle bombardment is limited to ~1500 Da. The objective of the present study was to evaluate NP-SIMS for the detection of up to two tagged proteins in membranes of extracellular vesicles, EVs. EVs are nanometric objects, 20-230 nm in size,[19] shed by cells mainly for signaling purposes.[20] Their size exemplifies the

challenge of protein studies at the level of individual moieties. We tested NP-SIMS on urine EVs where podocin expression may correlate with renal injury.[21] We also examined co-localization of two exosome marker proteins, CD81 and CD63.

5.2 Experiment and Methods

5.2.1 Sample Preparation

Model samples which approximate membrane surfaces were prepared using halide-containing small molecule tags conjugated to antibody (Ab) in order to test the application of NP-SIMS to analysis of single layers (figure 5.1). Halide-containing small molecule tags used in this study were erythrosine (iodide tag; EMP Biotech, Berlin, Germany), eosin (bromide tag; MarkerGene Tech, Eugene, OR) and 4,4′-bis-(1″,1″,1″,2″,2″,3″,3″-heptafluoro-4″,6″-hexanedion-6″-yl) sulfonylamino-tetraethyleneglycol-succinimidyl carbonate-o-terphenyl (BHHTEGST). BHHTEGST was synthesized[22] from the commercially available 4,4″-Bis(4,4,5,5,6,6,6-heptafluoro-1,3-dioxohexyl)-o-terphenyl-4′-sulfonyl chloride (BHHCT; AdipoGen, San Diego, CA). BHHTEGST was preferred to BHHTC in order to increase detection sensitivity of the fluorine tag. BHHTEGST is more soluble than BHHCT in aqueous solutions thus it was possible to enhance the tag to Ab ratio during the conjugation reaction. The detailed sample preparation and protocols of the tag molecules synthesis are in appendix A.

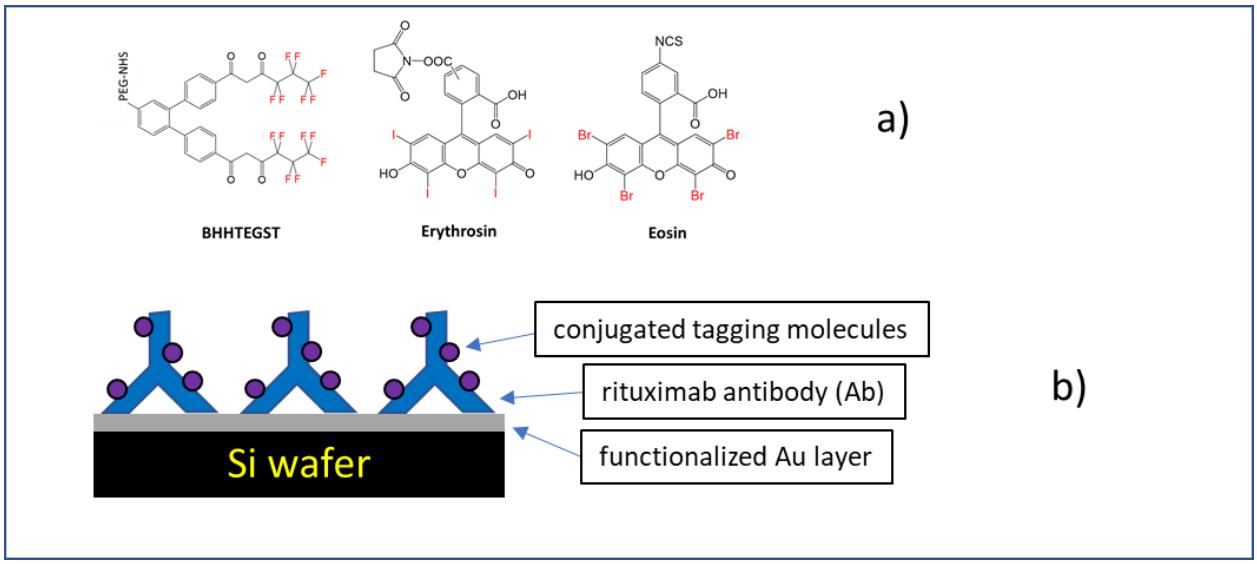

Figure 5.1. Tagging approach. a) Molecules conjugated to rituximab antibody (Ab) are BHHTEGST (fluoride tag), eosin (bromide tag) and erythrosine (iodide tag). b) Sketch of the model surface.

Briefly, BHHTEGST, erythrosine and eosin tags were conjugated to free amine groups on rituximab Ab via the active N-Hydroxysuccinimide (NHS), NHS, and isothiocyanate groups respectively. The conjugates were characterized by UV-Vis to confirm that the conjugation was successful (appendix A). Model surfaces consisting of single layers of covalently attached tag-Ab conjugates were prepared for each of the three tags. First, gold coated Si wafers were functionalized with Sulfo-NHS. Single layer model surfaces were analyzed as a reference sample to identify characteristic ions detected from each tag as well as their ion yield (number of ions detected per impact). The model surfaces were analyzed with NP-SIMS using the 1040 keV Au_{2800}^{8+} projectile (Figure 5.2). The sputter volume of each impact corresponds to the volume of ~3 tagged Abs.

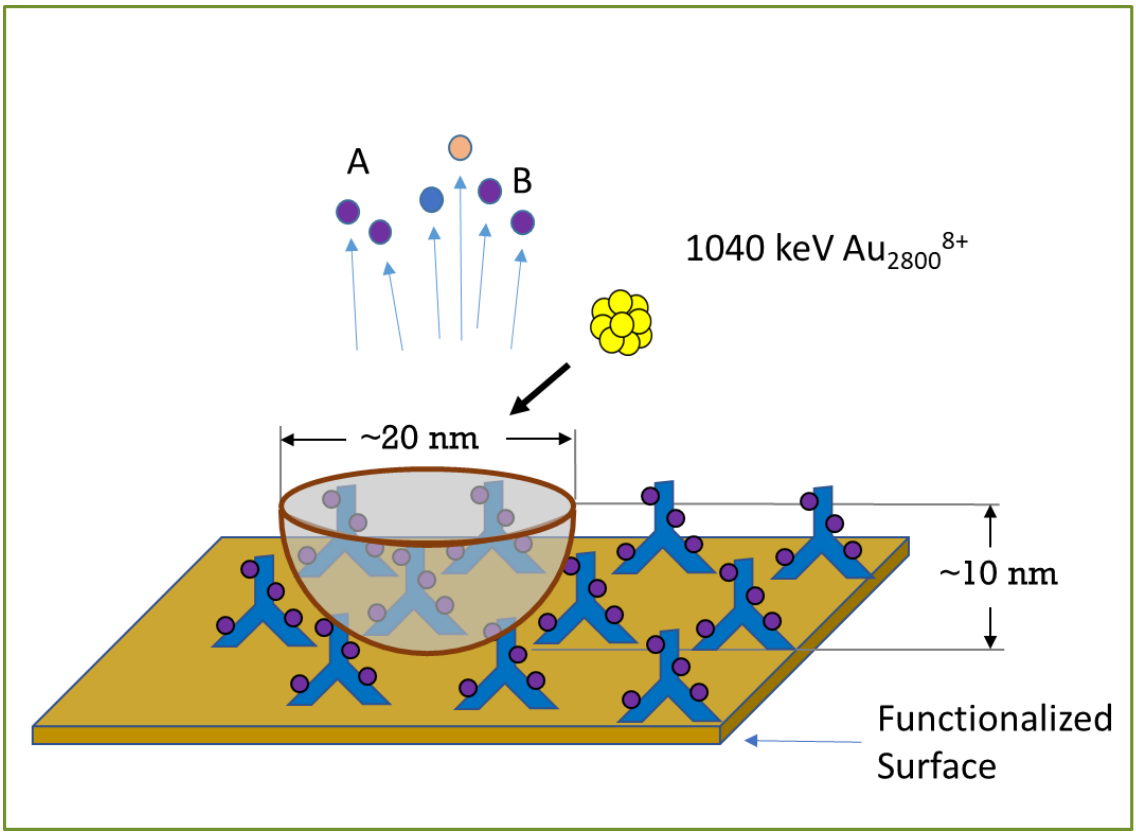

Figure 5.2. Sketch of emission volume stimulated by single projectile impact on a single tag model surface.

In a proof-of-concept experiment, EVs, attached via electrostatic interactions onto a poly-L-lysine (PLL) coated ITO glass slide, were tagged with erythrosine conjugated anti-podocin antibodies and analyzed (figure 5.3). One should note that the NP-SIMS variant used here requires vacuum conditions. In order to make the biological samples vacuum compatible, they were first fixed using Trump's fixative solution and dried using supercritical CO_2.[23] To test the detection of two tagged proteins in EV membrane simultaneously, exosome marker proteins CD63 and CD81 were tagged with erythrosine and BHHTEGST respectively. For this experiment, the tagged EVs were dried in 10^{-3} Torr vacuum for 1 hour.

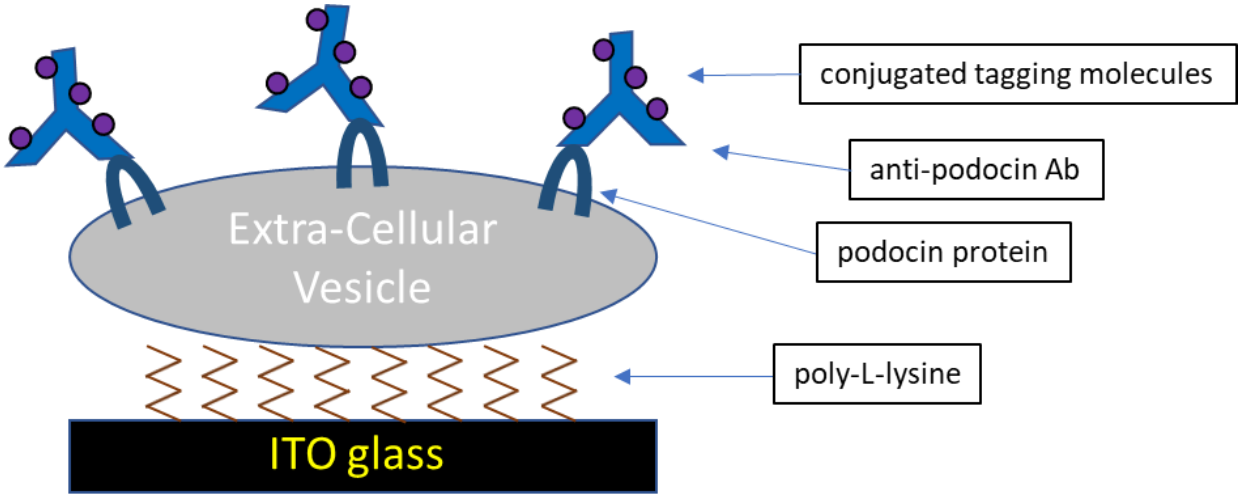

Figure 5.3. Sketch of EV sample design. Podocin on EVs was tagged with corresponding Ab conjugated to erythrosine tag.

5.2.2 Scanning electron microscopy (SEM)

SEM was used to confirm the presence of EVs on the surface. The SEM instrument used at Texas A&M University was JEOL JSM-7500F (Material Characterization Facility). This ultra-high resolution (~1 nm at 5 keV electron beam) field emission (FE) scanning electron microscope is equipped with a high brightness conical FE gun. Prior to imaging the sample was coated by Pt-Pd film (4nm). It is important to note that the sample was analyzed with NP-SIMS prior to SEM imaging. SEM instrument used at the Mayo Clinic was S4700 Hitachi.

5.2.3 Experimental device

Figure 5.4 shows a diagram of the custom NP-SIMS instrument.[24] The liquid metal ion source (LMIS) consists of a needle with a reservoir containing gold silicon eutectic.[25]

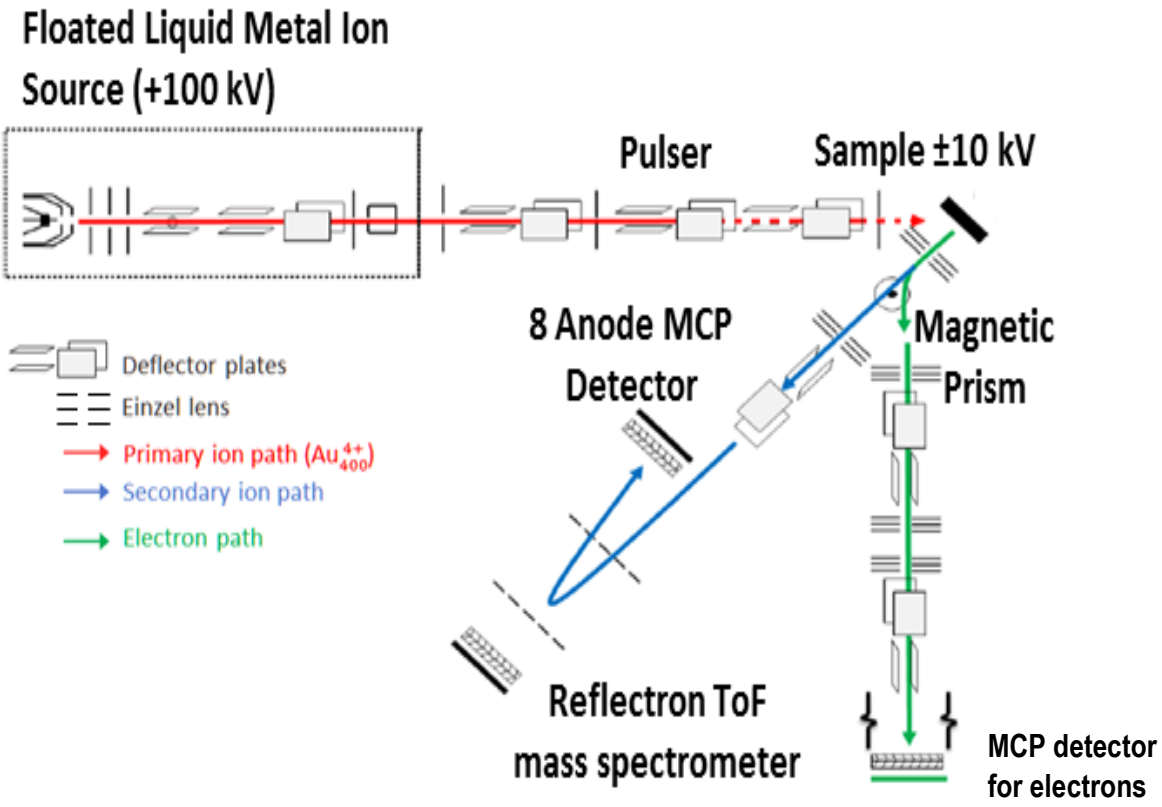

Figure 5.4. Schematic of custom-made NP-SIMS instrument.

The resulting projectiles are filtered using a Wien filter which selects Au clusters based on their velocity corresponding to a certain mass to charge ratio or number of Au atoms per charge (n/q). The projectile used in all presented experiments was 1040 keV Au_{2800}^{8+} (n/q=350)[26]. Emission volume generated by this projectile is ~20x20x10 nm^3.[26] A high voltage bias of 120 kV was used to accelerate the selected gold clusters and the resulting beam was pulsed at a frequency of 10-40 kHz, where each pulse contained 0.1 projectiles, separating each projectile in time and space resulting in individual projectiles. After each projectile impact the resulting SIs were extracted and analyzed with a reflectron time of flight, TOF, mass spectrometer. Due to the large number of SIs produced per impact, an 8-anode microchannel plate (MCP) detector was enabling the collection of multiple isobaric ions from each impact. All experiments were performed in the so called “negative SI detection mode.” In these experiments a magnetic prism diverted the emitted electrons which were then used as a start signal for the TOF measurement. Each sample was analyzed with 10^5 to 3.5×10^7 projectiles over an area 500 µm in diameter corresponding to 10^5 to 3.5×10^7 individual mass spectra. “Surface Analysis and Mapping of Projectile Impacts” (SAMPI©) is a custom mass spectrometry data analysis software and was used for mass spectrometry data analysis[27]. The analysis was performed in two modes: (1) identification of characteristic ions by analyzing the summation of all projectile impacts (total mass spectrum); (2) evaluating co-emitted ions by selecting an ion of interest and assessing the ions which were emitted and detected in the same projectile impacts (coincidence mass spectrum).

5.3 Results and Discussion

Experiments were carried out on the model samples containing single layers of tagged antibodies for each tag in order to approximate membrane conditions. Relevant mass spectra are shown in fig. 5.5-5.7 for samples that contain the rituximab antibody conjugated with erythrosine (iodide tag), eosin (bromide tag) and BHHTEGST (fluoride tag) respectively. Only the mass ranges containing characteristic ions are shown.

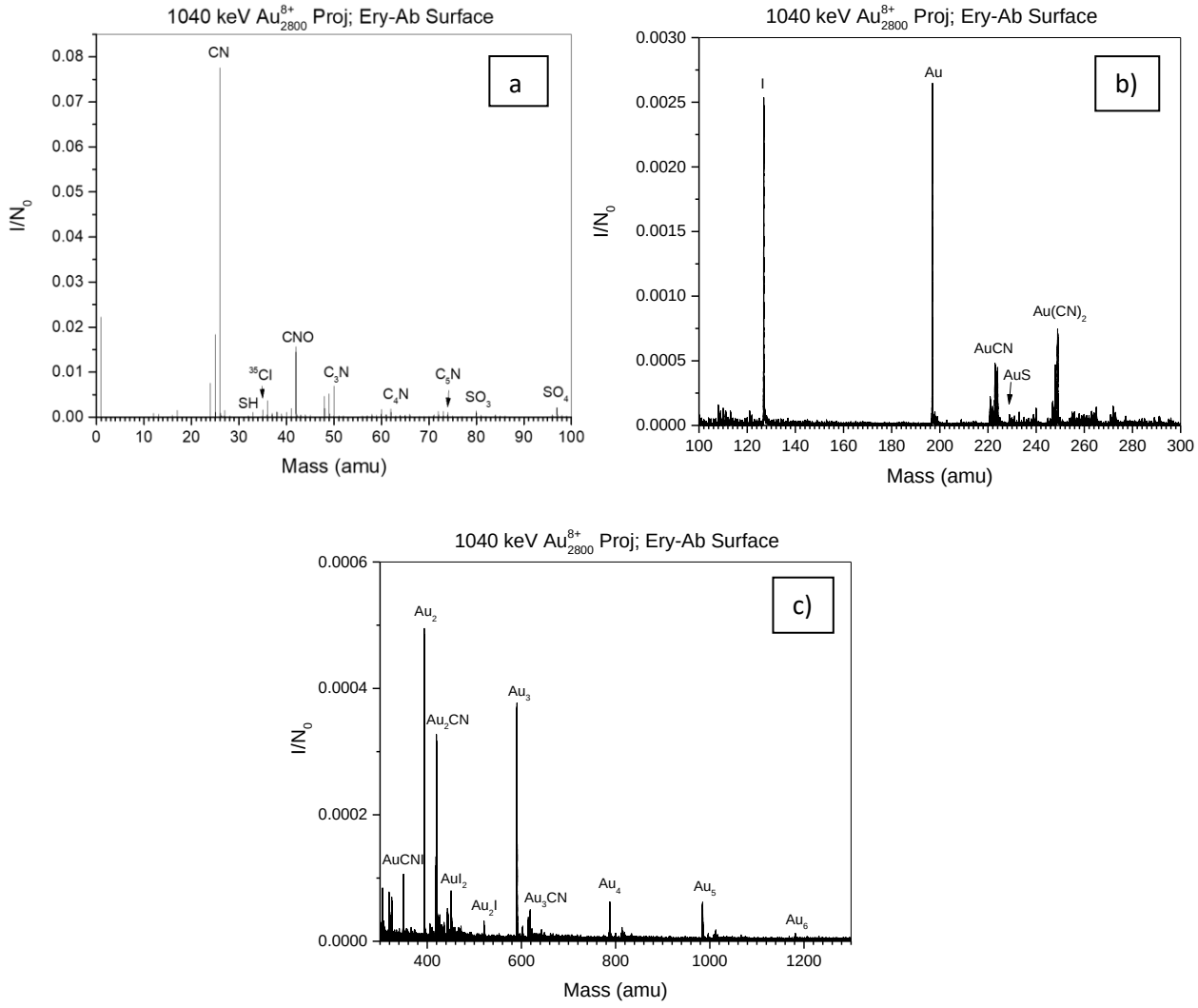

Figure 5.5a,b,c. The mass spectrum taken from the model sample of erythrosine-Ab conjugates (I tag) with direct covalent attachment on functionalized Au coated Si wafer. a) mass range of 0-100 amu, b) mass range of 100-300 amu, c) mass range of 300-1300 amu.

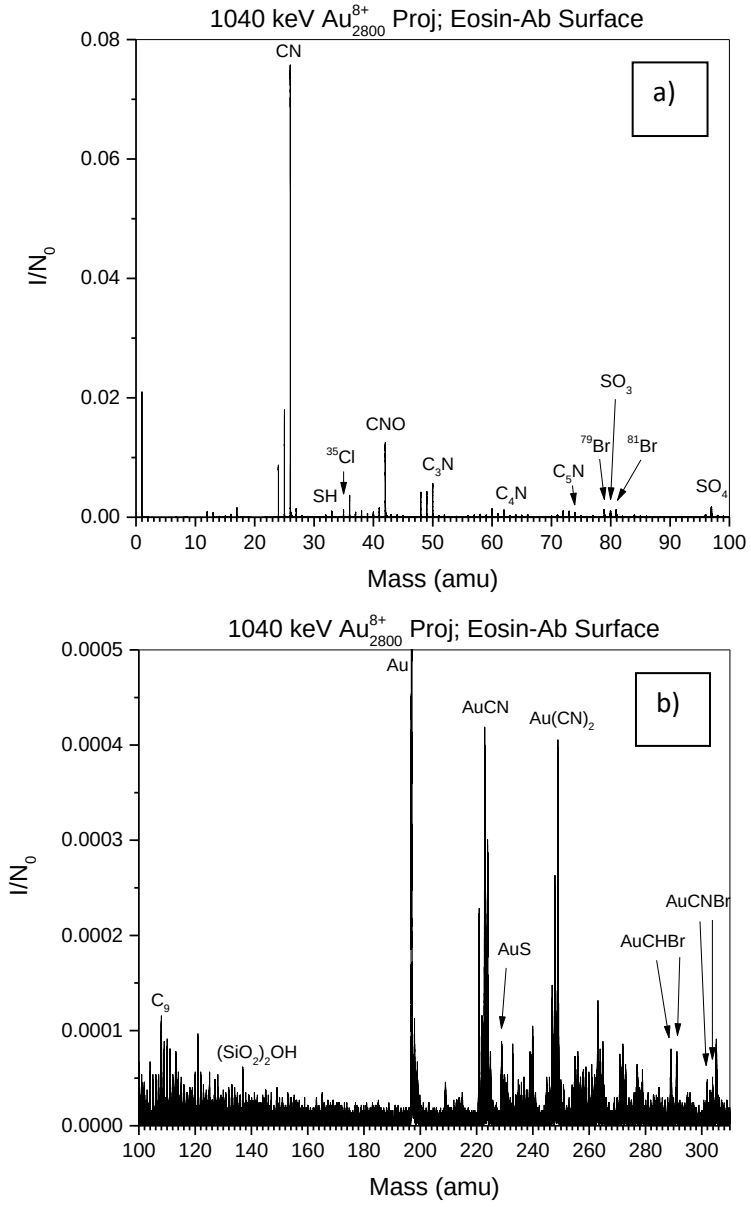

Figure 5.6a,b. The mass spectrum taken from the model sample of Eosin-Ab conjugates (Br tag) with direct covalent attachment on a functionalized Au coated Si wafer.

a) mass range of 0-100 amu, b) mass range of 100-310 amu.

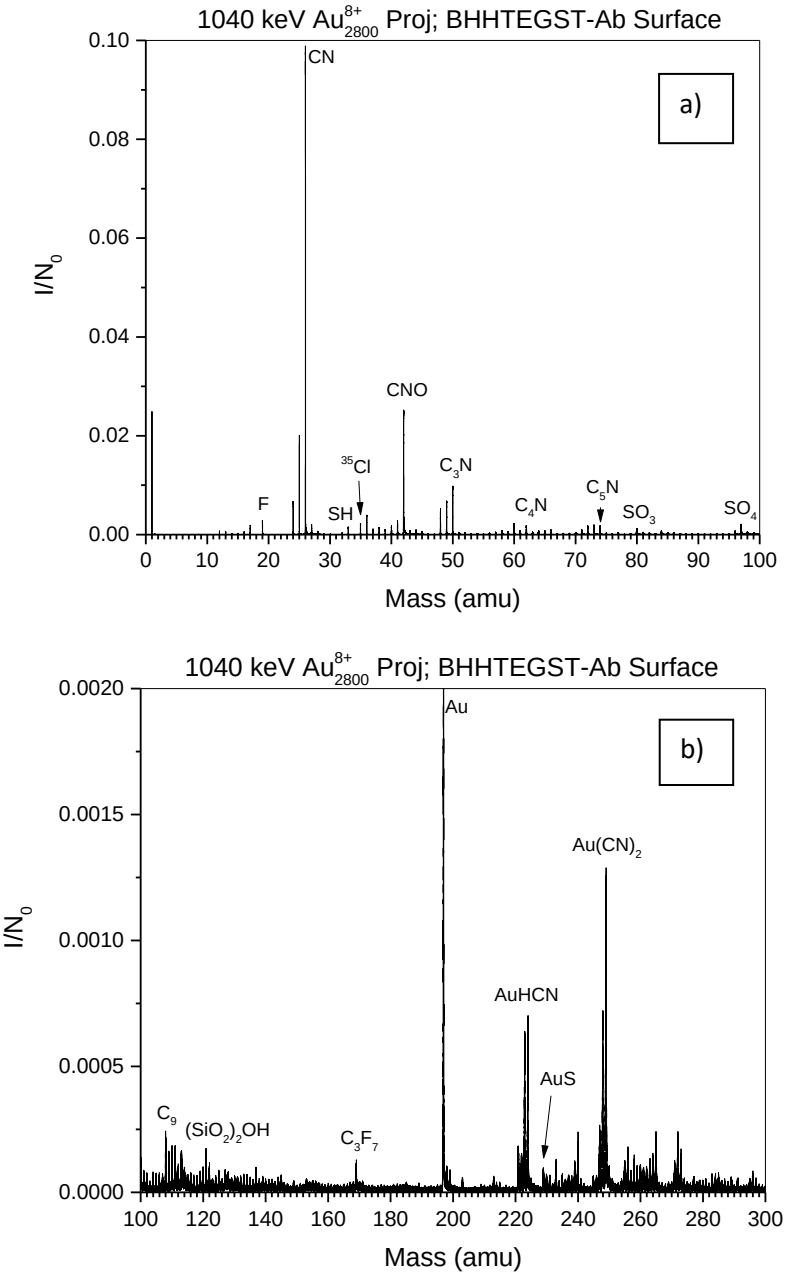

Figure 5.7a,b. The mass spectrum taken from the model sample of BHHTEGST-Ab conjugates (F^- tag) with direct covalent attachment on functionalized Au coated Si wafer.

a) mass range of 0-100 amu, b) mass range of 100-300 amu.

The list of characteristic ions detected and observed for each tag are listed in table 5.1.

Table 5.1. Characteristic ions detected for each tag conjugated to Ab.

Tag Conjugate	Characteristic Ions
Erythrosine-Ab	I^-, $AuCNI^-$, AuI_2^-, Au_2I^-
Eosin-Ab	$^{79}Br^-$, $^{81}Br^-$, $AuCHBr^-$, $AuCNBr^-$
BHHTEGST-Ab	F^-, $C_3F_7^-$

Some of the ions listed in table 5.1 are Au adducts. One should note that the emission of Au adducts is the result of an “in situ” process. In situ emission means that each single impact of an Au cluster, which is a donor of atoms and energy, initiates the synthesis of Au-containing adducts and their emission.[28] The ion yields (number of ions detected per impact) for halide ions originating from the tags are shown in table 5.2.

Table 5.2. Yields (ions detected per impact) for each halide ion on model single layer surfaces. The standard deviation is better than ±5% for all values of the measured yields shown.

	Y_I	$Y_{^{79}Br}$ $Y_{^{81}Br}$	Y_F
Erythrosine-Ab (I^- tag)	**0.25**	0.02 0.03	0.002
Eosin-Ab (Br^- tag)	0.001	**0.11** **0.11**	0.002
BHHTEGST-Ab (F^- tag)	0.002	0.02 0.04	**0.11**

In the case of fluoride and iodide, trace amounts of non-specific/interfering ions were detected for samples which do not have the corresponding tag. The ratio of yields of tag related F^- and I^- to non-specific F^- and I- was 55 and 125 respectively. The case of bromide is different. Peaks of bromide ions ($^{79}Br^-$ and $^{81}Br^-$) are interfered with peaks of phosphate related ions (PO_3^- and $H_2PO_3^-$) as seen from the nonspecific yields of 0.02-0.04 in table 5.2. For the model sample, the phosphate related ions are due to phosphate buffer residue. Anticipating the discussion concerning EVs, phosphate related ions can also originate from the membrane lipid fragments. In summary, BHHTEGST and erythrosine are viable tags for membrane surface analysis of biological samples. However, eosin is significantly interfered by phosphate-related ions and can only be used when phosphate-containing compounds are absent from the analyte.

Quantitative results from model single layers are needed to estimate the "decision limits"[29] of NP-SIMS for detecting tagged membrane samples. We have shown previously that the event-by-event bombardment-detection mode allows to determine the coverage of the surface by nano-objects.[28,30] Here the surface covered by the antibody molecules is given by the ratio of the number of impacts where 2 co-emitted SIs (e.g. F^- and C_3F_7) were detected, N_c, to the total number of projectiles impacting the surface, N_0. This ratio is referred to as the % surface coverage, k:

$$k\ (100\%) = \frac{N_c}{N_0} 100\% \qquad (5.1)$$

For erythrosine sample, the tag-related ions used were I^- and AuI_2^-. For eosin sample, the tag-related ions present were isotopes of bromide $^{79}Br^-$ and $^{81}Br^-$. For BHHTEGST sample tag-related ions used were F^- and $C_3F_7^-$. The experimental values obtained are listed in table 5.3. The coverages were 95%, 98% and 90% for erythrosine-Ab, eosin-Ab and BHHTEGST-Ab model surfaces respectively. The surface coverage for eosin-Ab is likely overestimated due to the interference discussed above.

Table 5.3. Surface coverages for each sample.

	Erythrosine-Ab: Co-emitted ions I^- and AuI_2^-	**Eosin-Ab:** Co-emitted ions $^{79}Br^-$ and $^{81}Br^-$	**BHHTEGST-Ab:** Co-emitted ions F^- and $C_3F_7^-$
surface coverage, *K*	95% ±3%	98% ±2%	90% ±2%

The method was applied to EVs where we labeled membrane podocin proteins with erythrosine and analyzed with NP-SIMS and SEM. In addition, there were two negative controls: one with untagged EVs, another with EVs absent. Representative scanning electron microscopy (SEM) micrograph of the EVs captured on the ITO substrate is shown in fig. 5.8. SEM micrographs for EV-only and no-EV negative control were obtained (see appendix).

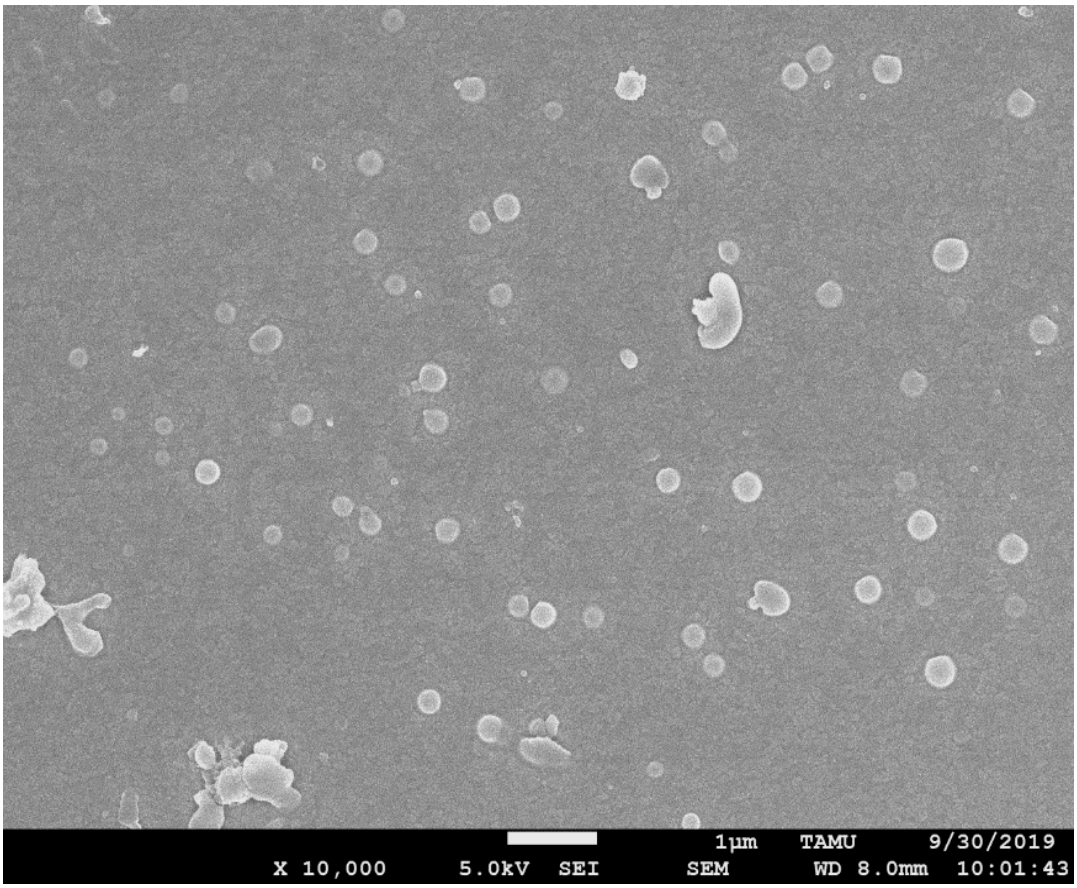

Figure 5.8. SEM micrograph of the tagged EV sample. The round shaped objects are EVs. The small crystals at the surface are likely salt inclusions.

The sample shown in fig. 5.8 was examined with NP-SIMS (prior to SEM). The mass spectrum obtained from the tagged podocin protein on the EV surfaces shows a clear iodide signal (fig. 5.9). The mass spectra from the negative control samples with untagged EVs and a functionalized ITO surface exposed to the tagged antibodies without EVs are shown in figure 5.9a. All three samples demonstrate the presence of iodide. However, the yields of I^- measured for the control samples were small (fig. 5.9b). The ratios of I^- yields, $Y/Y_{control}$ were ~30.

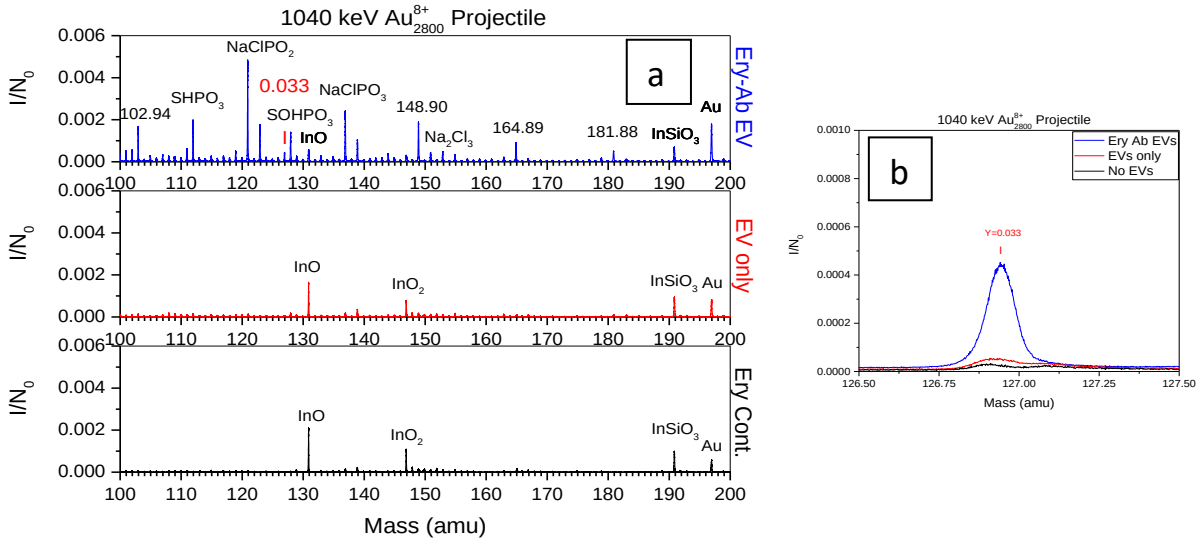

Figure 5.9 a,b. a) Mass spectra from the proof-of-concept EV experiment. The top (blue) mass spectrum is for EVs, which were tagged by erythrosine-Ab. The middle spectrum (red) represents EVs without tags (EV-only). The bottom spectrum is the control surface, which does not contain EVs. This sample was exposed to erythrosine with subsequent rinsing. b) Comparison of the peaks of I^- for all mass spectra.

Following the demonstration of detection of one tag in EVs, the next objective was to determine the feasibility of detecting two tagged proteins simultaneously. This experiment tests the viability of future co-localization studies of EV and cell membranes with NP-SIMS at the nanoscale. Three samples were analyzed: (1) EVs tagged with erythrosine (labeling CD63 protein) and BHHTEGST (labeling CD81 protein), (2) EVs tagged with BHHTEGST only (labeling CD 81 protein) and (3) untagged EVs (negative control). The results are presented in figure 5.10. For the fluoride ion, the ratio of yields of the two-tag sample to the EV only negative control was ~8. In the case of EVs tagged with BHHTEGST-only the ratio to the negative control was ~13. For the iodide ion, the ratio of yields of the two-tag sample which contains the erythrosine tag to the EV-only control was ~3. The ratio of yields was the same for the EVs tagged with BHHTEGST-only versus the EV-only negative control. All these ratios are above the “decision limit” value[29] of 3:1. SEM of parallel samples confirmed the presence of EVs (see supplementary materials). The 2-tag experiment demonstrates that it is possible to use BHHTEGST and erythrosine tags to study a system of two proteins of interest on membrane surfaces using NP-SIMS. In fact, assuming 10% surface area coverage by EVs estimated from the SEM image of the parallel sample (appendix), 250 of 8.5×10^5 projectile impacts on EVs detected both tagged CD63 and CD81 proteins co-localized within the same emission volume.

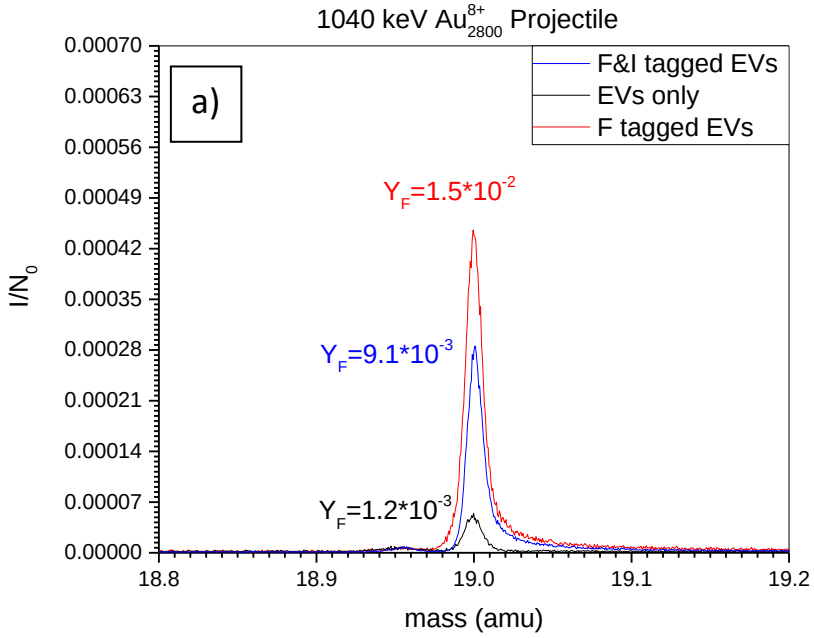

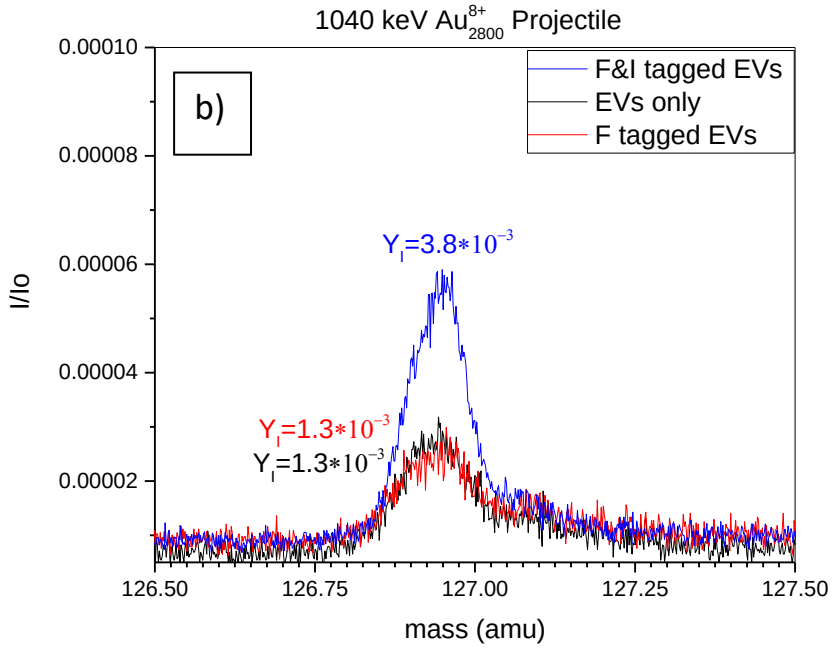

Figure 5.10a,b. Mass spectra of two-tag EV experiment. (a) Shows comparison of F^- peak for EVs tagged with BHHTGEST-antiCD81-Ab, EVs tagged with erythrosine-antiCD63-Ab and BHHTGEST tagged CD Anti-CD81 Ab and untagged EVs. (b) Comparison of the 3 samples listed above but for I^- peak.

The measured yield of I^- for the model erythrosine surface with 95% coverage of tagged Abs is 0.25 ions/impact. Thus, the yield, Y_{neat}, for 100% coverage would be 0.26. Let us estimate the "decision limit" for iodide tag at the surface based on signal-to-background ratio of 3:1.[29] Then the minimum detectable I^- yield, Y_{limit}, is 0.0045 (Table 5.2). The ratio Y_{neat}/Y_{limit} was 58, meaning we can detect up to 58 times fewer Ab tags than we have in a neat single layer case. The Ab cross-sectional area is between 73 nm^2 and 170 nm^2 depending on its orientation on the surface. Therefore, a fully covered single layer Ab surface has between 5600 and 13700 Abs per um^2. Taking into account the ratio, Y_{neat}/Y_{limit}, the minimal density of surface Ab that can be detected with NP-SIMS is between 96 and 236 Abs per μm^2. Considering probing depth of 10 nm, we can detect ~1% of tagged protein sample in a volume of 10^{-2} μm^3. The "decision limit" can also be calculated for the fluorine tag using the same formulas and the yields from the BHHTGEST-Ab model surfaces. The ratio Y_{neat}/Y_{limit} is 20 meaning it is possible to detect between 280 and 685 Abs per μm^2. This value corresponds to ~5% of tagged protein sample in a volume of 10^{-2} μm^3.

5.4 Conclusions

NP-SIMS in the event-by-event bombardment detection mode enables ultra-sensitive detection of I and F tagged membrane proteins. Detection is based on probing ~5% of the membrane material in a region 500 µm in diameter. Thus, the assay preserves most of the sample, enabling examination of the same specimen by other techniques such as SEM.

As described here, 2-tag detection via NP-SIMS represents an alternative to FRET-based[31] techniques. The space of application of NP-SIMS may be expanded with

a broader panel of tags. Indeed with detection based on mass spectrometry, the range of possible tags extends beyond fluorescent moieties. An intriguing prospect is offered by Rare-Earth metal atoms which can be chelated to organic molecules for subsequent binding to antibodies.

5.5 References

(1) D. R. Bandura, V. I. Baranov, O. I. Ornatsky, A. Antonov, R. Kinach, X. Lou, S. Pavlov, S. Vorobiev, J. E. Dick, S. D. Tanner, Anal. Chem. **81**, 6813 (2009).

(2) E. Hutter, D. Maysinger, Microsc. Res. Tech. **74**, 592 (2011).

(3) C. Lechene, F. Hillion, G. McMahon, D. Benson, A. M. Kleinfeld, J. P. Kampf, D. Distel, Y. Luyten, J. Bonventre, D. Hentschel, K. M. Park, S. Ito, M. Schwartz, G. Benichou, G. Slodzian, J. of Biol. **5**, 20 (2006).

(4) C. Chen, S. Zong, Z. Wang, J. Lu, D. Zhu, Y. Zhang, Y. Cui, ACS Appl. Mater. Interfaces **8**, 25825 (2016).

(5) M. Angelo, S. C. Bendall, R. Finck, M. B. Hale, C. Hitzman, A. D. Borowsky, R. M. Levenson, J. B. Lowe, S. D. Liu, S. Zhao, Y. Natkunam, G. P. Nolan, Nat. Med. **20**, 436 (2014).

(6) L. Keren, M. Bosse, S. Thompson, T. Risom, K. Vijayaragavan, E. McCaffrey, D. Marquez, R. Angoshtari, N. F. Greenwald, H. Fienberg, J. Wang, N. Kambham, D. Kirkwood, G. Nolan, T. J. Montine, S. J. Galli, R. West, S. C. Bendall, M. Angelo, Sci. Adv. **5**, eaax5851 (2019).

(7) S. G. Boxer, M. L. Kraft, P. K. Weber, Annu. Rev. Biophys. **38**, 53 (2009).

(8) M. L. Kraft, Front. Cell Dev. Biol. **10**, (2017).

(9) R. L. Wilson, J. F. Frisz, W. P. Hanafin, K. J. Carpenter, I. D. Hutcheon, P. K. Weber, and M. L. Kraft, Bioconjugate Chem. **23**, 450 (2012).

(10) M. M. Lozano, Z. Liu, E. Sunnick, A. Janshoff, K. Kumar, S. G. Boxer, J. Am. Chem. Soc. **135**, 5620 (2013).

(11) M. J. Eller, A. Vinjamuri, B. E. Tomlin, E. A. Schweikert, Anal. Chem. **90**, 12692 (2018).

(12) R. D. Rickman, S. V. Verkhoturov, E. S. Parilis, E. A. Schweikert, Phys. Rev. Lett. **92**, 047601 (2004).

(13) M. A. Park, K. A. Gibson, K. Quinones, M. A. Schweikert, Science **248**, 988 (1990).

(14) V. T. Pinnick, S. V. Verkhoturov, L. Kaledin, Y. Bisrat, E. A. Schweikert, Anal. Chem. **81**, 7527 (2009).

(15) M. J. Eller, S. V. Verkhoturov, E. A. Schweikert, Anal. Chem. **88**, 7639 (2016).

(16) A. B. Clubb, M. J. Eller, S. V. Verkhoturov, E. A. Schweikert, R. M. Anderson, R. M. Crooks, J. Vac. Sci. Technol., B: Nanotech. & Microelect.: Mat., Proc., Meas., & Phen. **34**, 03H104/1 (2016).

(17) C.-K. Liang, M. J. Eller, S. V. Verkhoturov, E. A. Schweikert, J. Am. Soc. Mass Spectr. **26**, 1259 (2015).

(18) C.-K. Liang, S.-T. Chang, S. V. Verkhoturov, L.-C. Chen, K.-H. Chen, E. A. Schweikert, Int. J. Mass Spectrom. **370**, 107 (2014).

(19) O. E. Bryzgunova, M. M. Zaripov, T. E. Skvortsova, E. A. Lekchnov, A. E. Grigor'eva, I. A. Zaporozhchenko, E. S. Morozkin, E. Ryabchikova, Y. B. Yurchenko, V. E. Voitsitskiy, P. P. Laktiono, PLoS ONE **11,** e0157566 (2016).

(20) G. Van Niel, G. d'Angelo, G. Raposo, Nat. Rev. Mol. Cell Biol. **19**, 213 (2018).

(21) S. I. Gilani, U. D. Anderson, M. Jayachandran, T. L. Weissgerber, L. Zand, W. M. White, N. Milic, M. L. Gonzalez Suarez, R. R. Vallapureddy, Å. Nääv, L. Erlandsson, J. C. Lieske, J. P. Grande, K. A. Nath, S. R. Hansson and V. D. Garovic, JASN **28**, 3363 (2017).

(22) N. Sayyadi, R. E. Connally, and A. Tryb, Chem. Commun. **52**, 1154 (2016).

(23) D. J. Hall, E. J. Skerrett, W. D. E. Thomas, J. Microsc. **113**, 277 (1978).

(24) J. D. Debord (2012). Evaluation of Hypervelocity Gold Nanoparticles for Nanovolume Surface Mass Spectrometry. Doctoral dissertation, Texas A&M University. Available electronically from http://hdl.handle.net/1969.1/148083.

(25) M. Benguerba, A. Brunelle, S. Della-Negra, J. Depauw, H. Joret, Y. Le Beyec, M. G. Blain, E. A. Schweikert, G. Ben Assayag, P. Sudraud, Nucl. Instrum. Meth. B: Beam Interac. Mat. Atoms **62**, 8 (1991).

(26) M. J. Eller, A. Vinjamuri, B. E. Tomlin, E. A. Schweikert, Anal. Chem. **90**, 12692 (2018).

(27) M. J. Eller, S. V. Verkhoturov, S. Della-Negra, and E. A. Schweikert, Rev. Sci. Instrum. **84**, 103706 (2013)

(28) M. J. Eller, M. Li, X. Hou, S. V. Verkhoturov, E. A. Schweikert, P. Trefonas, J. of Micro-Nanolith. MEMS, **18**, 23504 (2019).

(29) L. A. Currie, Anal. Chem. **40**, 586 (1968).

(30) S. Rajagopalachary, S. V. Verkhoturov, E. A. Schweikert, Nano Lett. **8**, 1076 (2008).

(31) S. Itoh, K. Mizuno, M. Aikawa, E. Aikawa, J. Biol. Chem. **293**, 4532 (2018).

6. METHODOLOGY FOR CO-LOCALIZATION

6.1 Introduction

Co-localization on the surface of molecules such as amino acids and nano-objects similar in size to proteins has been previously shown with NP-SIMS run in event-by-event bombardment detection mode. Among those studies, some focused on successfully detecting co-localized nanoparticles in the range of ~5 nm using the Au_{400}^{4+} projectile. However, so far there have not been any studies published which considered co-localized protein-sized nanoobjects in a single layer on the surface with NP-SIMS using the Au_{2800}^{8+} projectile. The emission volume of the Au_{2800}^{8+} projectile should enable to co-detect up to three tagged proteins in a single layer surface, which is impossible with the Au_{400}^{4+} projectile. This ability is crucial in order to make studies of protein-lipid raft complexes possible. On the one hand, we want to have nanoscale resolution to probe individual complexes, however, it is also important to probe a large enough nano-volume to detect co-emitted ions from more than one co-localized protein and perhaps even characteristic fragments of molecules such as lipids originating from associated lipid rafts. Thus, it is important to demonstrate the ability to study local inhomogeneity on the scale of individual tagged proteins in a single layer. In the present study we show the feasibility of detection of three tagged proteins simultaneously and examine limitation to homogeneity at the nanoscale.

6.2 Results and Discussion

Two cases are examined below that are critical for the aims presented above. The first case concerns three tags (eosin, erythrosine and BHHTEGST) conjugated to Ab and attached as a single surface layer (1:1:1 concentration ratio by Ab). It is a proof-of-concept experiment to determine the possibility of simultaneous detection of three co-localized tags from one projectile impact. Additionally, methodology to calculate the co-localization factor from experimental data is established.

For the second case, BHHTEGST chelated with Eu and Sm is used as a model of a concept where a single molecule becomes the tag base, while characteristic signal comes from the different chelated lanthanide atoms. In this way the same chemical and structural properties of the tag-Ab conjugates is maintained in order to overcome the problem of their inhomogeneous deposition at the nanoscale.

6.2.1 Three-tag experiment

With the three-tag model experiment, using the unique technique described above, we searched for impacts where all three ions characteristic to each tag were detected (Figure 6.1a).

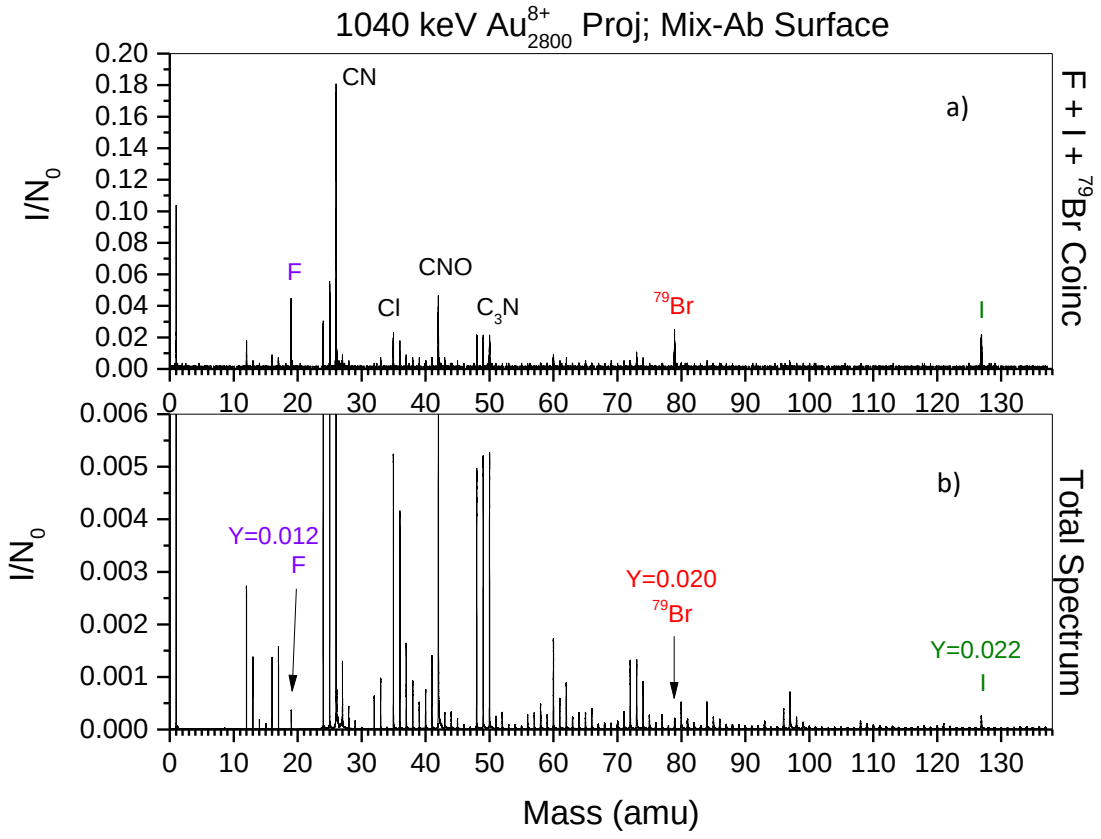

Figure 6.1. Mass spectrum of equimolar mixture model surface (three tags). a) Mass spectrum for selected projectile impacts where all three tags were detected (coincidence mass spectrum). b) Total mass spectrum for all projectile impacts. Probing area of each individual projectile impact was ~20 nm in diameter.

The mass spectrum demonstrates that we are able to detect three different co-localized conjugated tagged antibodies on the surface with a single projectile impact. The combination of these impacts is termed a “coincidence mass spectrum” where all ionized species co-emitted/detected with the tags are seen. The method allows the comparison of the total number of projectile impacts with the number of impacts on the surface sites where the tagging antibodies are co-localized. One should note that for the 1040 keV Au_{2800}^{8+} projectile, the probing volume of co-localization is 20×20×10 nm^3.[1] Thus, the information on the tagged Abs is obtained at the nanoscale (mesoscopic case), when the local concentration of antibodies experiences fluctuations. The goal is to investigate the influence of these fluctuations on the co-localization factor for the model antibody sample (Figure 6.1 b). Later this approach will be applied in order to correctly interpret the co-localization of the tagged Abs in biological samples such as cells and vesicles.

Let’s consider the total ensemble of projectile impact events, N_0, and the sub-ensemble of events, N^*. The sub-ensemble is defined as the events of projectile impacts, when the ions (e.g Br^- ions) are co-emitted/detected with F^- ions. The co-localization factor (definition and discussion below) can be computed using the concept of correlation coefficients for sub-ensembles.[2]

For the sub-ensemble N^*, the correlation coefficient for two tags (e.g. F^- and Br- ions from BHHTEGST and eosin respectively) is defined as:

$$K^* = \frac{Y^*_{F,Br}}{Y^*_{Br}} \frac{N^*}{n_F} = 1 \qquad [6.1]$$

where the coincidental yield, $Y^*_{F,Br} = \frac{I^*_{F,Br}}{N^*}$ (ions/impact), is the yield of co-emitted/detected ions of F^- and Br^-. The number of the events when the F^- ions were detected, n_F, corresponds to N^*, and computed from experimental total matrix of events.

The yield, Y^*_{Br},

$$Y^*_{Br} = \frac{I^*_{Br}}{N^*} \qquad [6.2]$$

is the effective yield of emitted/detected Br^- ions. The number of detected ions is denoted as I^*_{Br}, $I^*_{F,Br}$.

One can compute the co-localization factor, α, from the experimental data of co-emission using (6.1) and (6.2):

$$\alpha = \frac{Y_{Br}}{Y^*_{Br}} = \frac{I_{Br}}{I_{F,Br}} \frac{n_F}{N_0} \qquad (6.3)$$

where the yield, $Y_{Br} = \frac{I_{Br}}{N_0}$, is the total yield of Br^- ions, measured for the total ensemble of projectile impacts. The yield, Y^*_{Br}, is an effective yield for the sub-ensemble of impacts on nanometric surface areas, where the local concentration of both F-Ab and Br-Ab is increased.

For these areas $Y^*_{Br} > Y_{Br}$, thus the co-localization factor is $\alpha < 1$. For the surface, which is homogeneous at nanoscale, when the Ab local density fluctuations are absent or moderate, $\alpha \sim 1$. One should note that α is calculated from the experimentally measured intensities, which are obtained using the method of single projectile impacts. Conventional SIMS methods lack these capabilities.

An important feature of α is that this yield ratio (6.3) does not depend on ionization probabilities and detection efficiencies of the detected ions. Moreover, this

ratio does not depend on the number of molecules of BHHTEGST (fluoride tag), eosin (bromide tag) and erythrosine (iodide tag) conjugated to antibodies. However, the yield ratio (6.3) depends on the possible local nanoscale density fluctuations of antibodies with different tags.

The same approach can be used to calculate the co-localization factor of the three tagged Ab molecules. As was mentioned above, the differently conjugated antibodies were mixed equimolarly. The values of α measured for double and triple co-localizations are presented in Table 6.1.

Table 6.1. Co-localization factor for double and triple co-localizations of antibodies.

	F tag (BHHTEGST tagging molecules) and **Br tag** (Eosin tagging molecules)	**F tag** (BHHTEGST tagging molecules) and **I tag** (Erythrosine tagging molecules)	**Br tag** (Eosin tagging molecules and **I tag** (Erythrosine tagging molecules)	**F tag** (BHHTEGST tagging molecules), **I tag** (Erythrosine tagging molecules, and **Br tag** (Eosin tagging molecules)
Co-localization factor, α	0.65 ±0.02	0.70 ±0.02	0.62 ±0.02	0.42 ±0.02

The experimental co-localization factors, measured for the model Ab sample, show that the antibodies are not “ideally” co-localized. As mentioned above, this effect can be explained by the fluctuations of co-deposition of antibodies. Indeed, the antibodies are nano-objects ~10^3 nm^3 in size. The size of the probing volume (emission volume of a single impact) is just enough to probe three antibodies simultaneously. Thus, if three probed antibodies are related to two tags due to fluctuations, they will not be detected as a three-tag detection event. This effect was investigated previously,

when we examined the influence of the size of the emission volume on co-emission of molecules.[3] Table 6.1 shows that the co-localization factor, α, for two tags is ~0.7. For co-emission of three tags, the number is decreased to ~0.4, indicating a strong influence of fluctuations. We can consider a few sources of the density fluctuations of co-localized Ab molecules at the nanoscale. One source is a simple statistical variation of this density, which is regulated by a binomial distribution.[3] Another possible source is the effect of different degrees of hydrophobicity among the three different conjugates. Both sources regulate the density variations during direct attachment of the antibodies at the surface (covalent bounding). This model experiment is important for future work on cellular and EV samples, when the fluctuations of co-localization of tagged antibodies should be considered.

The data demonstrate that the three-tag model surface is inhomogeneous on the scale of emission area from a single projectile impact (~20 nm). Again, one of the reasons for the inhomogeneity is that the tags have different hydrophobicity due to differences in structure and functional groups, especially between BHHTEGST and erythrosine/eosin (Figure 6.1a). Hydrophobicity plays a role in self-organization of the conjugates on the surface during model surface preparation. The surfaces were prepared using a microfluidic device. As the NHS-activated functionalized surface is incubated with the tagged conjugates, their self-organization on the surface is in part determined by interactions between each other.[4,5] This process leads to inhomogeneity of the resulting attached layer. The effect will be lessened on biological surfaces since antibody-antigen interaction is significantly stronger and tags will have greater affinity to other tags rather than to the membrane surface. To remove the effect, we assembled a

monolayer of a single chelate capable of carrying lanthanide metal tags. Specifically, BHHTEGST is used as base which is chelated making the hydrophobicity of all tags similar. The most important aspect of using lanthanide metal chelates is the potential for tag multiplexing (discussion below). In the following section we show results from a model experiment with Eu and Sm chelated BHHTEGST antibody conjugates.

6.2.2 BHHTEGST-Ab lanthanide chelated tags

As was mentioned above, in order to generate a tag library with the same chemical and structural properties while also opening up a prospect of multiplexing, BHHTEGST-based Ab conjugates were chelated. Electron structure of the lanthanide atoms allows their chelation to organic molecules such as BHHTEGST (Figure 6.2).

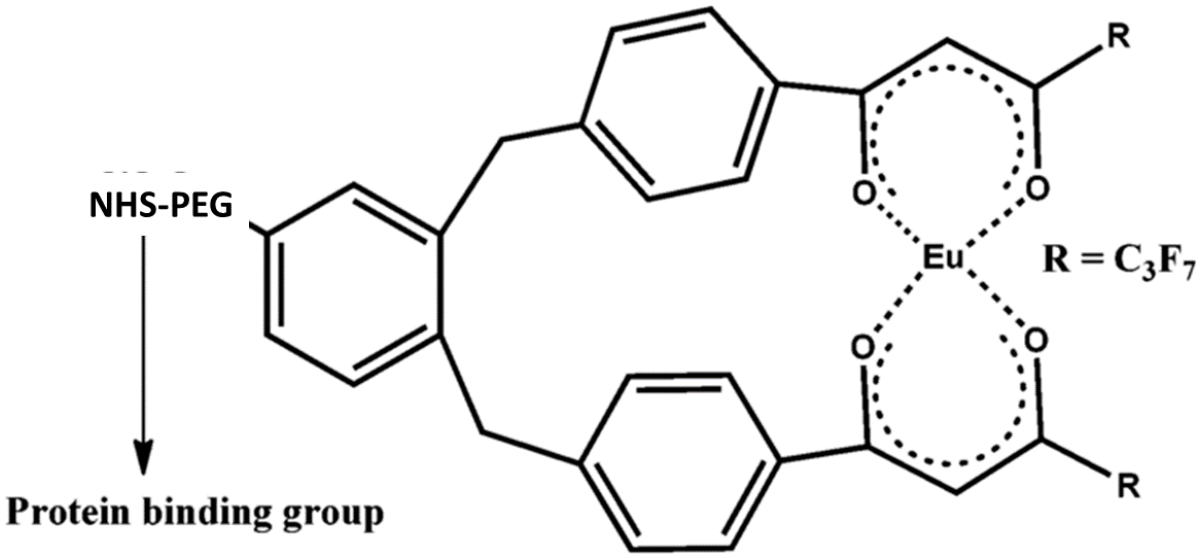

Figure 6.2. Sketch of BHHTEGST molecular tag chelated with Eu atom.

As shown in Figure 6.2, the two diketone groups on BHHTEGST chelate a metal ion, which can then be used as a mass tag for NP-SIMS. The advantage of using lanthanides is that they are a group of 14 metals (55 isotopes) with similar chemical properties. Thus there is a library of labels for multiplex tagging. To make a model Ab surface, a few problems had to be overcome. We found that the most efficient way of Ab tagging is to conjugate the Ab with a BHHTEGST molecule first and then perform the chelation procedure (details and protocols are in the Appendix A). The solubility of La-BHHTEGST-Ab conjugates in solution was optimized by varying the buffer conditions (see Appendix A).

As mentioned in chapter 4, there are commercially available lanthanide metal tags that use a chelated X8 polymer scaffold for conjugation of tag to Ab (Maxpar, South San Francisco, CA). Each polymer chain contains ~22 lanthanide ions with 3-4 polymers conjugated to each Ab. However, each polymer is 7 nm long and thus the tag density of the conjugates is much lower than in the case of BHHTEGST-Ab chelates that are densely packed on the Ab surface. This was confirmed by a model experiment (data shown in chapter 4).

For the first experiments, two lanthanide elements were used, Eu and Sm. The samples consisting of a molecular layer of rituximab antibody conjugated to BHHTEGST molecules, which are chelated with lanthanides. Sample 1 and 2 contain Eu and Sm chelated BHHTEGST respectively. For sample 3, Eu-BHHTEGST-Ab and Sm-BHHTEGST-Ab were prepared and mixed equimolarly by antibody concentration. Then the chelates were covalently attached to functionalized Au coated Si wafers (see Appendix A for procedure).

The characteristic peaks from the mass spectrum of sample 1 (Eu-BHHTEGST-Ab) are shown in Figure 6.3. For this sample the tag-related ions are F^-, $C_3F_7^-$ and $^{151}EuF_4^-$. Eu has two isotopes ^{151}Eu (abundance 47.81%) and ^{153}Eu (abundance 52.19%). Both are presented in mass spectra as molecular ions of EuF_4^-. The molecular fragments are the result of rearrangement of the diketone side of the tag in the projectile impact zone. The peak of $^{153}EuF_4^-$ is interfered by the peak of AuS^- (origin of Au adducts is discussed above). However, the peak of $^{151}EuF_4^-$ is distinct and can be considered for tag analysis (Figure 6.3c). An investigation of the mass spectrum shows that a good candidate for Sm-BHHTEGST tag analysis is the peak of $^{152}SmF_4^-$ (Figure 6.4c). The ^{152}Sm isotope has an abundance of 26.75%. In future experiments, to increase sensitivity, an isotopically enriched Sm should be used.

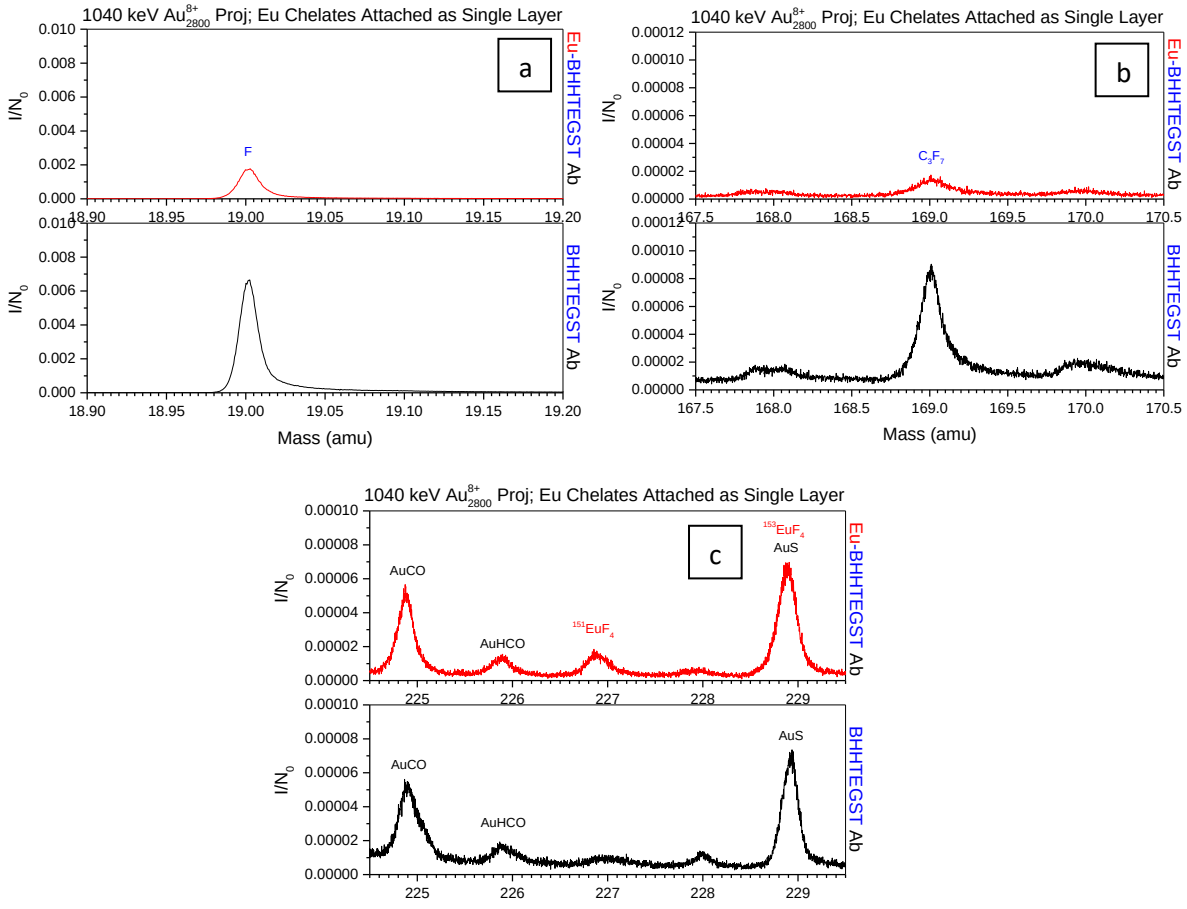

Figure 6.3a,b,c. Selected areas of the mass spectrum of sample 1 (Eu-BHHTEGST-Ab). The characteristic peaks of chelated tag molecules (top, red) are compared with the peaks from the same mass areas for control sample (bottom black) of BHHTEGST-Ab (no chelated Eu).

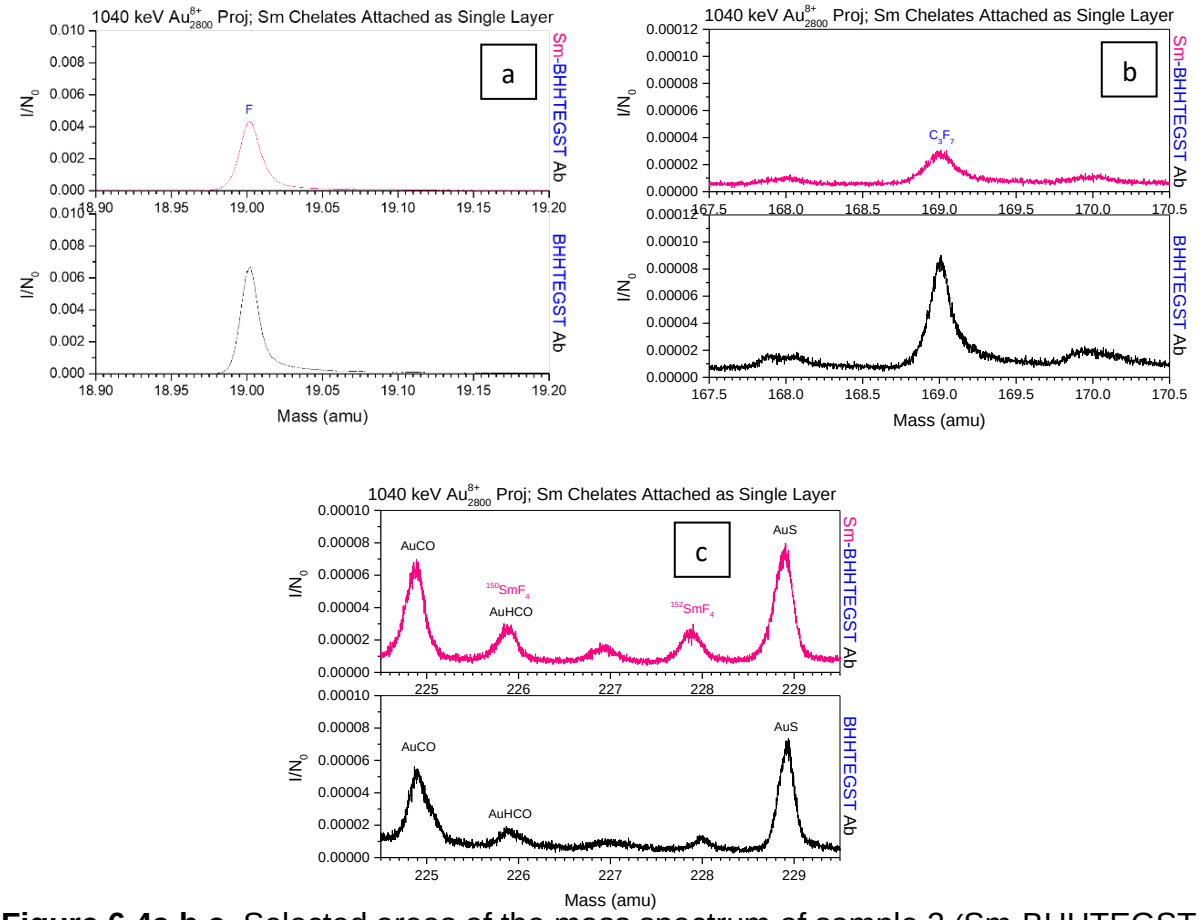

Figure 6.4a,b,c. Selected areas of the mass spectrum of sample 2 (Sm-BHHTEGST-Ab). The characteristic peaks of chelated tag molecules (top, pink) are compared with the peaks from the same mass areas for control sample of BHHTEGST-Ab (no chelated Sm).

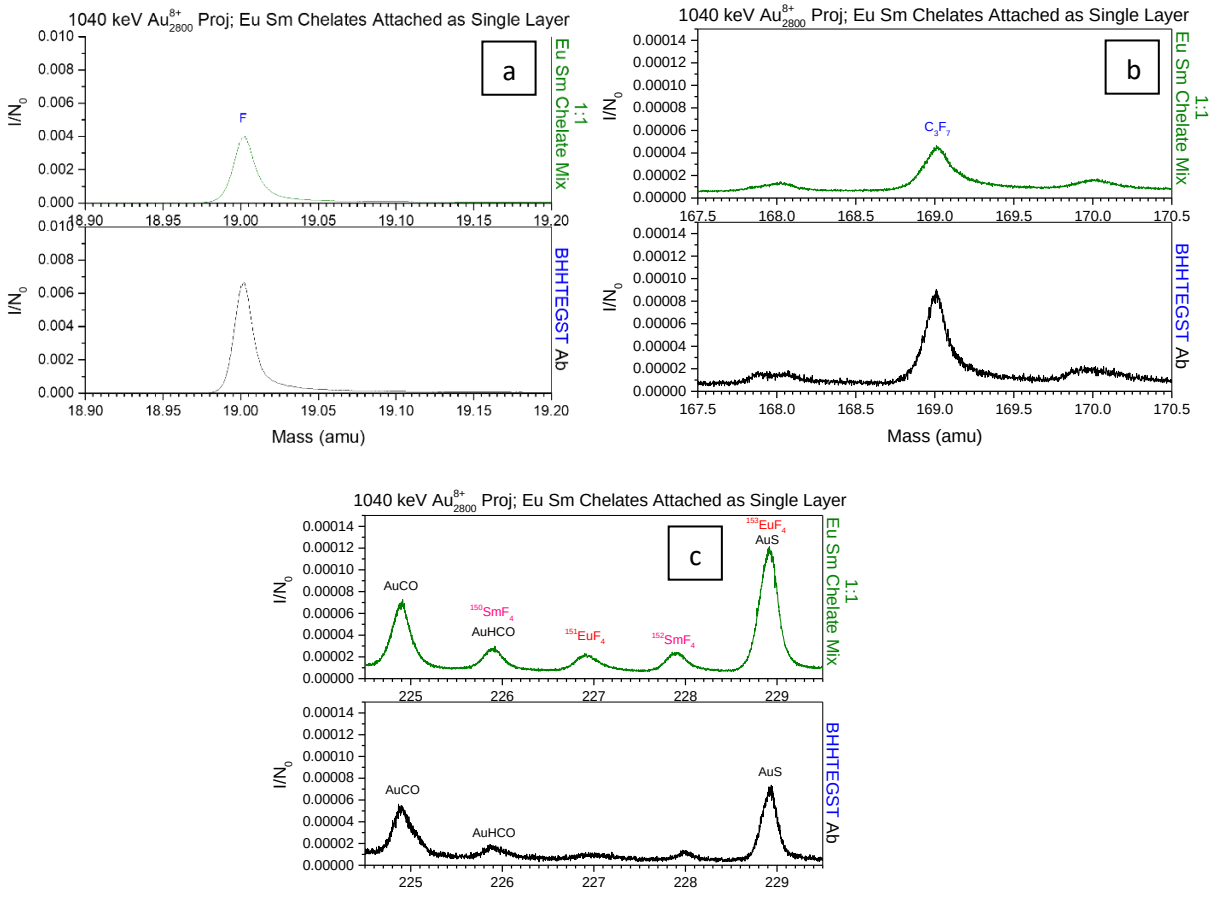

Figure 6.5a,b,c. Selected areas of the mass spectrum of sample 3 (mix of Eu-BHHTEGST-Ab and Sm-BHHTEGST-Ab). The characteristic peaks of chelated tag molecules (top, green) are compared with the peaks from the same mass areas for the control sample (bottom, black) of BHHTEGST-Ab (no chelated Eu and Sm).

Now we turn to the experiment with mixed Eu-BHHTEGST-Ab and Sm-BHHTEGST-Ab tags. The mass spectrum is shown in Figure 6.5a,b,c. The mass spectrum contains the peaks of both tagging ions of $^{151}EuF_4^-$ and $^{152}SmF_4^-$ (Figure 6.5c). The question to be addressed is: what is the Ab coverage of the substrate? For the mixed sample, there is an additional question related to the problem of detection of co-localized chelated tag-Ab molecules. Specifically, what is the co-localization factor for Eu-Ab and Sm-Ab molecules?

The surface coverage by tagged antibodies was calculated using the selection of events of co-emission of Ab ions (F^- and $C_3F_7^-$). This method was described in the experimental chapter. The coverage coefficients for all three samples are presented in Table 6.2.

Table 6.2. Coverage coefficients, K, for samples 1-3.

	Sample 1: Eu-BHHTEGST-Ab	**Sample 2:** Sm-BHHTEGST-Ab	**Sample 3:** mix Eu-BHHTEGST-Ab and Sm-BHHTEGST-Ab
coverage coefficient, *K*	40% ±4%	72% ±2%	49% ±2%

Table 6.2 shows that the model samples are covered by sub-monolayers of the tagged antibodies. The interesting case is the mixed sample. The calculated of co-localization factor, α, is 0.14 (calculation procedure described above: section “Three-tag experiment”) while the coverage of the sample by mixed antibodies is 49% (Table 6.2). Let’s consider two scenarios of Ab deposition on the surface. For the first scenario, the antibodies deposited with preference for island growth, thus half of the surface is not

covered. For this case, the co-localization factor of Eu-Ab and Sm-Ab should be ~0.5 (Equation 6.3).

If the antibodies are attached randomly at the surface (second scenario), the number of co-localized molecules in a single probing volume (20×20×10 nm^3) is smaller than in an organized layer. One might expect ~1.5 Ab molecules in the probed volume. The measured co-localization factor of 0.14 matches this scenario, indicating that random attachment is preferred.

6.3 Conclusions

The uniqueness of the method used is that the secondary ions are recorded separately from each emission volume of ~20×20×10 nm^3, which allows stochastic probing of the sample area. In the present study the effective probing area for the model surfaces is ~5% of the total, indicating comprehensive analysis of the surface nano-domains, which contain the co-localized surface proteins tagged with BHHTEGST, eosin and erythrosine (three-tag experiment). For the first time, we were able to detect three co-localized tagged proteins in a single layer with a single nanoparticle projectile impact. Due to comparable nano-volumes of the probed zone and the analyte, we were able to show local density fluctuations of the three different tagged Abs on the scale of the emission volume. We attribute the nanoscale inhomogeneity to differences in hydrophobicity between the tags which affect their attachment to the surface during preparation. The fluctuations were absent in the chelated lanthanide BHHTEGST tag case since their chemical and physical properties are the same. The present results, taken together with previous work analyzing co-localization of nano-objects using the Au_{400}^{4+} projectile, which has a smaller emission nano-volume, shows that it is possible

to tailor the nano-particle projectile to the specific biological sample and problem being investigated.

Regarding lanthanide tags, the signal from characteristic ions was not sufficient for direct application to biological samples. It should be recalled that for EuF_4^- and SmF_4^- tag-related ions, their emission depends on probability of their *in-situ* synthesis via recombination in the vicinity of the chelated molecule (fast, *in situ* picosecond chemistry).[6] Metal tetrafluorides have high electron affinities,[7,8] thus high ionization probabilities. However, the probability of synthesis reduces the emission of EuF_4^- and SmF_4^-. It is possible to enhance sensitivity by using isotopically enriched lanthanide metals corresponding to peaks which were free from interference such as ^{151}Eu and ^{152}Sm. It is important to note that the electron affinities of lanthanide atoms are small, thus negatively charged atomic ions of Eu and Sm are not detectible for the relevant concentrations of tag.

The ionization probabilities of lanthanide atoms are low in the positive ion detection mode as well,[9] however, it is possible to increase detection sensitivity via laser post-ionization of ejected metal atoms. Indeed, the ionization potentials of lanthanide atoms are relatively small, ranging from 5.43 eV for Lu to 6.25 eV for Yb. They can be ionized using commercially available ArF excimer lasers with 193 nm wavelength (6.42 eV). For these post-ionization parameters, the ionization probability is expected to be sufficiently enhanced.[10]

6.4 References

(1) M. J. Eller, A. Vinjamuri, B. E. Tomlin, E. A. Schweikert, Anal. Chem. **90**, 12692 (2018).

(2) R. D. Rickman, S. V. Verkhoturov, E. S. Parilis, E. A. Schweikert, Physical Review Letters **92**, 047601/1 (2004).

(3) C.-K. Liang, S. V. Verkhoturov, L.-J. Chen, E. A. Schweikert, International Journal of Mass Spectrometry **334**, 43 (2013).

(4) D. K. Schwartz, Annual Review of Physical Chemistry **52**, 107 (2001).

(5) A. J. Patel, P. Varilly, S. N. Jamadagni, H. Acharya, S. Garde, and D. Chandler, PNAS **108**, 17678 (2011).

(6) C. Guillermier, S. Della-Negra, E. A. Schweikert, A. Dunlop, G. Rizza, International Journal of Mass Spectrometry **275**, 86 (2008).

(7) S. V.Kuznetsov, M. V.Korobov, L. N. Sidorov, L. N. Savinova, V. A. Shipachev, V. N. Mit'kin, International Journal of Mass Spectrometry and Ion Processes **87**, 1 (1989).

(8) G. L. Gutsev, A. I. Boldyrev, Journal of Inorganic Chemistry **34**, 304 (1989).

(9) M. L. Yu, K. Mann, Physical Review Letters **57**, 1476 (1986).

(10) A. V. Samartsev, C. Heuser and A. Wucher, Surf. Interface Anal. **45**, 87 (2013).

7. CONCLUSIONS

The aim of this study was to enhance nanoscale analysis relevant for toxicology research, specifically the detection of proteins in membranes. The experimental effort focused on the development of NP-SIMS run in the event-by-event bombardment-detection mode. This technique combines the versatility of mass spectrometry with the ability to probe nano-volumes. Two key objectives for the successful application of NP-SIMS were to achieve: (1) analyte detection sensitivity suitable for nano-volume assays and (2) analyte selectivity. Previous NP-SIMS experiments with Au_{400}^{4+} projectiles demonstrated the feasibility of nanoscale detection of low weight (100s of Da) moieties in tissues,[1,2] confirming again the well-known limit in SIMS of effective ionization of organic moieties up to ~1500 Da. The latter limitation imposes a tagging requirement for most proteins. Furthermore, the detection sensitivity required for membrane analysis called for a more efficient projectile than Au_{400}^{4+}. The present study shows achievements on both extreme sensitivity and selectivity.

First, a tagging approach needed to be selected that would meet the following main requirements: (1) satisfactory detection sensitivity in the context of single nano-projectile impacts for single layers of a protein sample; (2) the size of the tag comparable to the size of antibody used to label the surface proteins. Commercially available lanthanide-chelated polymer scaffold and metal nanoparticle tags did not meet the detection sensitivity requirements to be applicable to “actual” biological membranes. The former tag did not have sufficient density of lanthanide atoms while the latter tag’s cap shielded ion emission from the nanoparticle core. An alternative tagging approach

which avoided these two issues by having halide-containing small molecule tags concentrated directly on the surface of the labeling Ab of interest was finally chosen.

The next study focused on confirming the ability to detect tagged proteins in a single layer using NP-SIMS with individual Au_{2800}^{8+} projectile impacts. Indeed, single layers of Ab, tagged with F/Br/I-containing small molecules, were detected. The characteristic ion signal was sufficient for analysis of biological membranes where the total amount of protein on the surface is expected to be smaller by at least an order of magnitude compared to the model surfaces.

The objective of the following experiment was to prove the capability of NP-SIMS to detect a particular protein on a biological membrane using the successfully tested Ab-sized halide tags. We were able to show detection of erythrosine (iodine) labeled podocin on a sub-single layer of EVs. Most importantly co-localization of two tagged proteins (CD63 and CD81) on a sub-single layer of EVs was also successfully demonstrated. These results document zeptomole detection sensitivity.

Having confirmed the ability to detect tagged proteins with single Au_{2800}^{8+} nanoparticle projectile impacts on a biological target, the next objective was to develop methodology for co-localization analysis of multiple tagged proteins in a single layer using model surfaces. For the first time, we were able to detect three tagged co-localized proteins in a single layer model surface from a single nanoparticle projectile impact. Considering the nano-volume probed is comparable to the nano-volume of the analyte, we were able to show local density fluctuations of the three different tagged Abs on the 20 nm level. These fluctuations were caused primarily by the differences in the hydrophobicity and chemical properties among the three tags that induced

nanoscale inhomogeneity during the process of their attachment on the surface. To confirm the above finding, lanthanide-chelated BHHTEGST tags were tested. The tags have the same chemical and physical properties because they have a single molecule as its base (BHHTEGST). The only difference between the tags is the chelated lanthanide atom. Indeed, a model surface, containing a single layer of Eu and Sm chelated BHHTEGST tags conjugated to Ab, lacked the local density fluctuations observed in the three-tag experiment above on the scale of the emission nano-volume from single impacts with the Au_{2800}^{8+} nanoparticle projectile.

The lanthanide-chelated BHHTEGST tags offer important advantages over other tags discussed in the present study. The advantages include the prospect of extensive multiplexing along with the fact that different lanthanide-chelated BHHTEGST tags have the same chemical and physical properties and the only difference is the identity of the chelated metal. Unfortunately, the ionization probabilities of lanthanide atoms are low for both negative and positive ion detection modes.[3] In the negative ion detection mode, the detected characteristic ions are lanthanide tetrafluorides. Lanthanide tetrafluorides have high electron affinities,[4,5] however, the necessary step of in situ synthesis via recombination reduces their emission. It should be noted that Au_{2800}^{8+} nano-projectile impacts stimulate abundant sputtering of neutral species including lanthanide atoms. The sputtered atoms of lanthanides (range of ionization potentials from 5.43 eV for Lu to 6.25 eV for Yb) can be ionized using commercially available ArF excimer laser with 193 nm wavelength (6.42 eV). For these post-ionization parameters, the ionization probability is expected to be sufficiently enhanced.[6] Laser pulses must be synchronized

with single projectile impacts, getting the duty cycling of ~2000 events/s for the co-localization experiment.

The future outlook of NP-SIMS includes exploring possibilities of a more efficient projectile. The projectile parameters that can be adjusted include kinetic energy and projectile size. 12 MeV Au_{400}^{4+} has been shown[7] to increase the yields of characteristic tag ions from similar tag-Ab conjugates by an order of magnitude compared to the 520 keV Au_{400}^{4+}. The energy of 30 keV per atom in the case of the 12 MeV Au_{400}^{4+} projectile implies that the mechanism of ejection is still via generation of a high-density collision cascade but with larger sputtered volume with a crater up to 100 nm in diameter. Alternatively, one can increase the sputtered volume by using a more massive projectile with larger momentum. As the amount of analyte sputtered in a single impact increases so does detection sensitivity but at the cost of decreased lateral resolution and vice versa. In fact, the projectile, and by extension volume of emission, can be tailored to the size of the co-localized analyte being studied, detection sensitivity and the lateral resolution desired.

In addition, it is possible to supplement the information on nanoscale co-localization of tagged proteins by mapping the location of the individual projectile impacts on the sample surface. A similar custom SIMS instrument at the Schweikert laboratory which uses single C_{60}^{2+} projectiles has demonstrated the capability to map individual impacts with ~1.2 μm lateral resolution.[8,9] Briefly, it uses a magnetic prism to direct the secondary electrons emitted from each impact toward an emission electron microscope to determine its location on the sample surface. The custom NP-SIMS instrument used in the present study is being upgraded with an additional analysis

chamber in the same beamline of the Au-Si eutectic LMIS. The new analysis chamber will have the electron emission microscope required for the mapping capability. Moreover, it is expected that the lateral resolution will be improved to the sub-micron range compared to the C_{60} instrument because the new analysis chamber will be vibrationally isolated.

If the technical challenges described above can be overcome and multiplexing capability is extended through post-ionization of chelated lanthanide tags along with the ability to map the location of projectile impacts with sub-micron lateral resolution, then NP-SIMS will be positioned to offer unique insights into biological and toxicological applications such as nanoscale co-localization of proteins inside particular protein-lipid raft nano-domains on cell and EV membranes.

7.1 References

(1) F. A. Fernandez-Lima, J. Post, J. D. DeBord, M. J. Eller, S. V. Verkhoturov, S. Della-Negra, A. S. Woods, E. A. Schweikert, Anal. Chem. **83**, 8448 (2011).

(2) F. A. Fernandez-Lima, J. D. DeBord, E. A. Schweikert, S. Della-Negra, K. A. Kellersberger, M. Smotherman, Surf. Interface Anal. **45**, 294 (2013).

(3) M. L. Yu, K. Mann, Physical Review Letters **57**, 1476 (1986).

(4) S. V. Kuznetsov, M. V. Korobov, L. N. Sidorov, L. N. Savinova, V. A. Shipachev, V. N. Mit'kin, International Journal of Mass Spectrometry and Ion Processes **87**, 1 (1989).

(5) G. L. Gutsev, A. I. Boldyrev, Journal of Inorganic Chemistry **34**, 304 (1989).

(6) A. V. Samartsev, C. Heuser and A. Wucher, Surf. Interface Anal. **45**, 87 (2013).

(7) T-L. Lai, D. Jacquet, I. Ribaud, S. Bilgen, B. Mercier, G. Sattonnay, M. J. Eller, D. Verkhoturov, E.A. Schweikert, L. H. G. Tizei, F. Shao, S. Della Negra, JVST B (accepted for publication).

(8) S. V. Verkhoturov, M. J. Eller, R. D. Rickman, S. Della-Negra, and E. A. Schweikert, J. Phys. Chem. C **114**, 5637 (2010).

(9) M. J. Eller, S. V. Verkhoturov, S. Della-Negra, and E. A. Schweikert, Review of Scientific Instruments **84**, 103706 (2013).

APPENDIX

Maxpar commercial polymer scaffold tagging

Isotopic Ln metal ion tags are loaded onto X8 polymers (Maxpar) via pentetic acid (DTPA) as shown on Figure 1. The polymers contain maleimide caps that bind free sulfhydryl groups on the antibodies. Each antibody is conjugated to ~3-4 polymer chains containing ~22 Ln ions placing the total number of tags at ~80. For the model experiment the conjugated antibodies are attached onto the surface of a Silicon wafer functionalized by (3-Aminopropyl)-triethoxysilane and glutaraldehyde.

BHHTEGST synthesis (fluorine-based tag)

The method was developed by Sayyadi N. *et al*. and the full detailed protocol can be found in their publication (Sayyadi, N. *et al*. RSC. 2015). Briefly, a PEG-NHS group is added to the sulfonyl chloride group of BHHCT.

Ab-tag monolayer experiment (Gold surface)

*** Antibody (Anti-mouse IgG, Sigma-Aldrich, M8642-5X1MG)**

- 1 mg/mL prepared in 0.1 M Bicarbonate buffer

- pH 8.5 for BHHTEGST and Erythrosine / pH 9.3 for Eosin-ITC

- 100 μL was used for the tag conjugation

*** Erythrosine-NHS (AF-01140D025.0-001, Generon, UK)**

- Prepared in DMF at 1.12 mM concentration

- 10 μL was added to the 100 μL Ab solution, 1h reaction at RT

- After the reaction, the Ab-tag conjugates were purified using Zeba™ Spin Desalting Columns (7K MWCO, 0.5 mL) for two times with 0.1 M Bicarbonate buffer at pH 7.4

*** Eosin-ITC (45245-50MG, Sigma-Aldrich)**

- Prepared in DMF at 1.12 mM concentration

- 10 μL was added to the 100 μL Ab solution, 1h reaction at RT

- After the reaction, the Ab-tag conjugates were purified using Zeba™ Spin Desalting Columns (7K MWCO, 0.5 mL) for two times with 0.1 M Bicarbonate buffer at pH 7.4

*** BHHTEGST**

- Prepared in DMF at 7.6 mM concentration

- 10 μL was added to the 100 μL Ab solution, 2h reaction at RT

- After the reaction, the Ab-tag conjugates were purified using Zeba™ Spin Desalting Columns (7K MWCO, 0.5 mL) for two times with 0.1 M Bicarbonate buffer at pH 7.4

*** Preparation of three Ab-tags for gold surface conjugation**

- Single tag : 20 μg/mL in 0.1 M Bicarbonate buffer (pH 7.4)

- Triple tags : Mix 60 μg/mL of each Ab-tag and make final concentration at 20 μg/mL in 0.1 M Bicarbonate buffer (pH 7.4)

- Treat the Ab-tag solutions to the EDC/NHS surface and incubate 2h and washed with bicarbonate buffer and DI water.

Ab-Erythrosine labeling on EV experiment

*** Antibody**

- Anti-podocin Ab IgG (Dr. Vesna's custom Ab)

- 5 mg/mL prepared in 0.1 M Bicarbonate buffer (pH 8.5)

- 100 μL was used for the tag conjugation

*** Erythrosine-NHS (AF-01140D025.0-001, Generon, UK)**

- Prepared in DMF at 5.6 mM concentration

- 10 μL was added to the 100 μL Ab solution, 1h reaction at RT

- After the reaction, the Ab-tag conjugates were purified using Zeba™ Spin Desalting Columns (7K MWCO, 0.5 mL) for two times with 0.1 M Bicarbonate buffer (pH 7.4)

*** Tag treatment to the EV-immobilized surface**

- Ery-Ab tag was prepared in 0.1 M bicarbonate buffer (pH 7.4) containing 2% BSA at 20 μg/mL concentration

- Incubate 1h and washed using 0.1 M bicarbonate buffer (pH 7.4) and PBS

- Treat Trump's fixative (~30 min) and dried using super-critical CO2 method.

Labeling of exosome with Erythrosine and BHHTEGST

***Reagent**

-Trump's fixative

-100 mM sodium bicarbonate buffer pH 7.4

-2% BSA in 100 mM sodium bicarbonate buffer pH 7.4

-10 mM sodium phosphate buffer (no salt) pH 7.4

***Load exosome to the Ab-coated device**

-To the antibody coated (and BSA-blocked) device, add the purified exosome

-Incubate for 1h (at least)

-Wash the device with 2% BSA solution (in 0.1 M SBC, pH 7.4)

***Labeling with antibody conjugates**

-By using NanoDrop, measure the antibody concentration of Erythrosine-conjugated antibody. Based on the concentration of Erythrosine antibody conjugates, assume the concentration of antibody of BHHTEGST conjugates.

-Dilute the antibody conjugates at 15 μg/mL of final concentration (single label and mixed label) using 2% BSA solution

-Add antibody conjugates to the device and incubate for 1h (at least)

-Wash the device with 2% BSA, 0.1M SBC, and 10 mM phosphate buffer sequentially

***Fixing the sample**

-Detach the PDMS device and dip the ITO glass to the Trump's fixative solution

UV-Vis Characterization of Conjugated Tags

*** NanoDrop™ One/One^{C} Microvolume UV-Vis Spectrophotometer (Thermo Scientific^{TM})**

*** Settings for Eosin/Erythrosine conjugation calculation**

Tag	Coefficient (1/mole-cm)	Wavelength (nm)	260 nm correction	280 nm correction
Eosin-ITC	83,000	521	0.47	0.28
Erythrosine-NHS	82,500	527	0.98	0.52

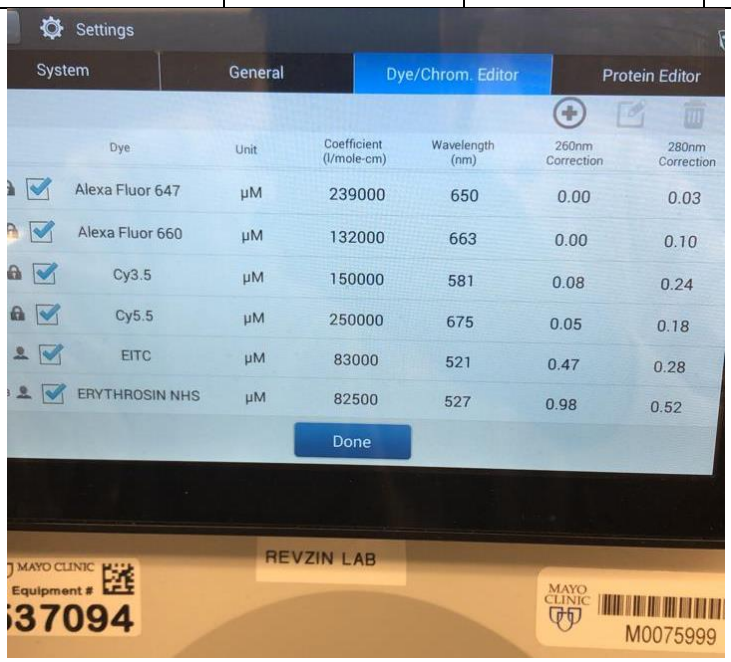

*** For the BHHTEGST, the values cannot be applied to the Nanodrop. So I measured the absorbance at 280 nm and 330 nm. Then, with the molar extinction coefficient value of BHHTEST (31,400 $M^{-1}cm^{-1}$)[1] and Invitrogen's equations [2], I calculated the conjugation yield for BHHTEGST-Abs.**

[1] A novel biocompatible europium ligand for sensitive time-gated immunodetection

https://doi.org/10.1039/C5CC06811H

[2] Calculate dye:protein (F/P) molar ratios

http://tools.thermofisher.com/content/sfs/brochures/TR0031-Calc-FP-ratios.pdf

SEM Imaging

SEM micrographs of the erythrosine tagged EV sample and the two negative controls:

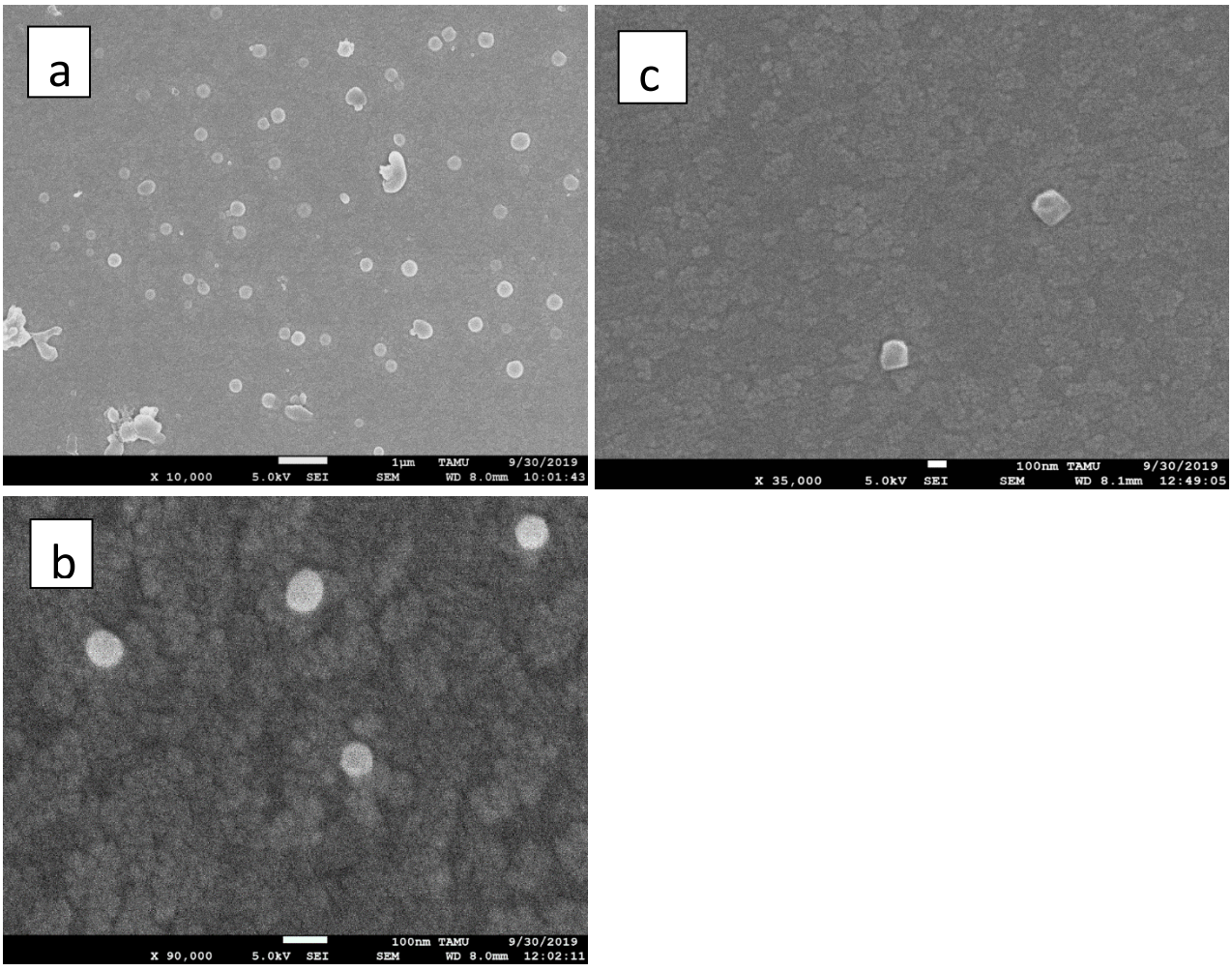

(a) SEM micrograph of the tagged EV sample. The round shaped objects are EVs. The small crystals at the surface are salt inclusions. (b) SEM micrograph of EV-only untagged sample. (c) SEM micrograph of no-EV negative control. Sample contains rare salt inclusions only (angular objects) without any EVs. SEM images were taken at Material Characterization Facility (Texas A&M University).

SEM micrograph of the parallel sample of erythrosine and BHHTEGST tagged EVs:

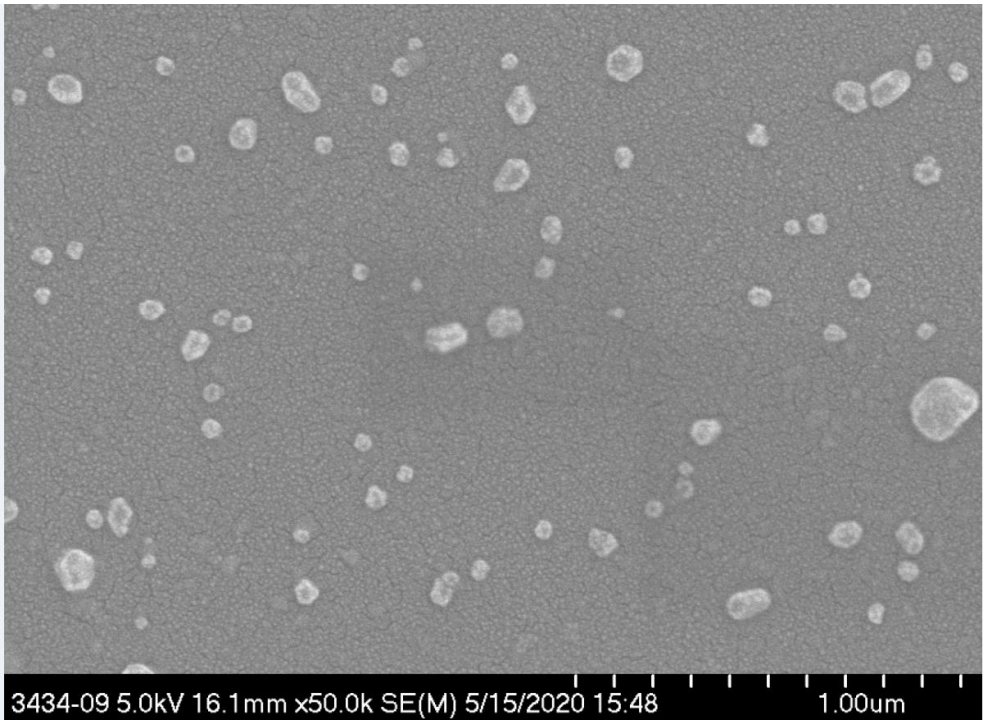

SEM image was taken at Mayo Clinic.